CHARACTERIZATION OF MICROEXPLOSION PHENOMENA OF METHANOL-GLYCEROL MIXTURES

A Thesis

by

GE-YI FAN

Submitted to the Office of Graduate and Professional Studies of
Texas A&M University
in partial fulfillment of the requirements for the degree of

MASTER OF SCIENCE

Chair of Committee,	Jorge L. Alvarado
Committee Members,	Kalyan Annamalai
	Alex (Gwo-Ping) Fang
Head of Department,	Andreas A. Polycarpou

August 2014

Major Subject: Mechanical Engineering

ABSTRACT

Due to the fast growth of biodiesel production capacity, the amount of glycerol has increased rapidly. Furthermore, the supply of glycerol has exceeded the demand needs in the market. In addition, there is a great demand for finding other new applications and ways to discard glycerol in an environmental friendly manner. One of innovative methods is to use glycerol as a liquid fuel in cogeneration and power generation. If it used properly, it could reduce the demand for conventional fossil fuels in those applications. However, glycerol has a very low vapor pressure and relatively high flash point values when compared to diesel and biodiesel. Therefore, ways to disperse and combust glycerol droplet should be researched. Recently, researchers have revealed that microexplosion occurs in binary fuel mixture droplets under specific temperatures since droplets consist of two liquids with different boiling point values. This phenomena can lead to higher combustion efficiency and a reduction of NO_x emissions even when combusting glycerol-based mixtures.

In this research, microexplosion phenomena of methanol-in-glycerol mixtures have been studied using a high speed camera and an acoustic sensor system. A Fast Fourier Transform (FFT) algorithm has been used to analyze the collected data using Matlab to understand frequencies of microexplosion. The main goal of this study is to find the highest probability of microexplosion occurrence under the certain temperatures and to understand the relationship between frequencies of microexplosion and droplet size. Methanol-in-glycerol mixtures with 5%, 10%, and 15% methanol were prepared and

tested in a microexplosion chamber. Also, water-in-glycerol mixtures with 50% water were mixed and compared with the results of methanol-in-glycerol mixtures. Droplet sizes were controlled at 230 μm and 130 μm using nanoparticle based coatings to be able to understand the effect of discrete droplet size on microexplosion properties.

The results indicate that temperature has a strong effect of the probability of microexplosion. Furthermore, bigger droplet size (230 μm) depicts higher probability of microexplosion occurrence than 130 μm droplets. In addition, the frequencies of microexplosion were measured under the temperature with the highest microexplosion probability. Furthermore, droplets with higher concentration of methanol exhibit higher microexplosion frequency. Size of droplet is also a significant factor that affects frequencies with smaller droplets exhibiting higher frequencies. Future studies will consider smaller droplets and other fuel mixtures.

DEDICATION

This thesis is dedicated to my family, Mr. Kuang-Huan Fan, Mrs. Hsien-Mei Fan-Lai, Mr. Yang-Fu Fan, Mrs. Pei-Chi Sung and Mr. Pu-Hsien Fan for their love and support through my life.

ACKNOWLEDGEMENTS

The outcome of this research required a lot of guidance and support. First, I would like to express my deep appreciation to my committee chair, Dr. Jorge L. Alvarado. Without his persistent support, this research would not have been possible. I am extremely grateful to him for giving me an opportunity to participate in this project. Also, I would like to thank two committee members, Dr. Kalyan Annamalai and Dr. Alex (Gwo-Ping) Fang, for their kind assistance.

In addition, I would like to thank Hyungseok Nam for teaching me to conduct the experiment and answering my questions. I am also thankful for my best friends, Andy Chen, Yu-Che Cheng, Timo Lai, Pei-Chung Huang and Jerry Liao for their encouragement.

Finally, I wish to express my sincere gratitude to my family, Mr. Kuang-Huan Fan, Mrs. Hsien-Mei Fan-Lai, Mr. Yang-Fu Fan, Mrs. Pei-Chi Sung and Mr. Pu-Hsien Fan, for giving me constant encouragement and support.

NOMENCLATURE

T	Sampling interval [s]
f_s	Sampling frequency [Hz]
$V_{ellipse}$	Volume of ellipse [m^3]
r_{sphere}	Radius of sphere [m]
$u\ (x\ ,t)$	Displacement of the plane of particle [m]
F	Constant total net force [N]
$\Delta t'$	Time interval over the impulse force [s]
m	Constant mass of the object [kg]
K	Microexplosion strength
M	Total mass of droplet including oil and water [kg]
J	Bubble nucleation rate [$1/m^3s^1$]
R_0	Initial radius of emulsion droplet [m]
R_1	Radius of emulsion kernel when oil membrane is formed [m]
k	Boltzmann's constant [1.3808×10^{-23} J/K]
h	Plank's constant [6.6261×10^{-34} J·s]
r_{cr}	Critical diameter of a vapor embryo [m]
n_T	Number of potential nucleation sites per unit volume

Greek symbols

ϕ	Volume fraction of water in an emulsified oil
θ	contact angle
$\gamma_{solid\text{-}gas}$	surface tension between solid and gas (dyne/cm)
$\gamma_{solid\text{-}liquid}$	surface tension between solid and liquid (dyne/cm)
$\gamma_{liquid\text{-}gas}$	surface tension between liquid and gas (dyne/cm)

Acronyms

EIA	US Energy Information Administration
CO_x	Carbon Monoxide
NO_x	Nitrogen Oxides
SO_x	Sulfur Dioxide
FFT	Fast Fourier Transform
GHG	Greenhouse Gases
AE	Acoustic Emission
SNR	Signal-to-Noise Ratio
ASP	Analog Signal Processing
DSP	Digital Signal Processing
ADC	Analog-to-Digital Converter
DFT	Discrete Fourier Transforms
GM	Methanol-in-Glycerol
GW	Water-in-Glycerol

PFI	Programmable Function Interface
DAQ	Data Acquisition

TABLE OF CONTENTS

Page

Page

LIST OF FIGURES

Page

Page

Page

LIST OF TABLES

Page

1. INTRODUCTION

Environmental issues related to energy production and uses continue to create concerns among users and producers alike. In addition, people around the world have started to find ways to protect the earth we live and to conserve natural resources that will run out eventually. With improvements in technology, the quality of living is better than before. However, damage to environment still is a concern in many parts of the world. Climate change, air pollution and limited natural resource are all important issues related to the environment, and people are trying to find out adequate solutions to these problems. Fuels derived from hydrocarbon are a major energy source in the world. However, it is a scarce natural resource and strongly associated with production of greenhouse gases. According to the US Energy Information Administration (EIA), the source of the primary energy consumption in 2012 were petroleum (36%), natural gas (26%), coal (20%), renewable energy (9%) and nuclear electric power (8%). The consumption of hydrocarbon fuel was over 75% of all the available energy source.

Hence, finding alternative sources of hydrocarbon fuel has become an important topic across the world. Renewable energy sources such as biofuel, wind power, solar power and geothermal energy have regained the attention of many stakeholders across the world. Renewable energy comes from natural sources and can replace conventional hydrocarbon fuels in many different areas. Also, it is considered a sustainable source of energy, which could never run out if managed adequately. At the present the consumption of renewable energy is just over 10% of total energy consumption in the world, but the

usage is still increasing due to increase awareness of their eco-friendliness and high energy density potential. Renewable energy sources not only decrease dependence on fossil fuels but also reduce harmful emissions such as carbon dioxide (CO_2), nitrogen oxides (NO_x), sulfur dioxide (SO_2) and soot when taking into account the whole production cycle. Therefore, renewable energy has less impacts on the environment compared to hydrocarbon fuels.

Biodiesel has already become one of alternative energy sources produced from vegetable oil, animal oil, tallow and used cooking oil. Biodiesel is made by the process of transesterification, which converts vegetable oils to fatty acid methyl esters (biodiesel) and glycerol (by-product). In general, 10% volume of the initial oils are transformed into glycerol. Because glycerol is almost colorless and clear liquid, it can be used in many areas such as foods, beverages, health care, cosmetics and other industrial applications. Due to the fast growth of biodiesel production capacity, the amount of glycerol has increased rapidly. Furthermore, the supply of glycerol has exceeded the demand needs in the market [1]. In addition, there is a great demand for finding other new applications and ways to discard glycerol in an environmental friendly manner. One of innovative methods is to use glycerol as a liquid fuel in cogeneration and power generation [2]. If it is used properly, it could reduce the demand for conventional fossil fuels in those applications. However, glycerol has a very low vapor pressure and relatively high flash point values when compared to diesel and biodiesel. Therefore, ways to disperse and combust glycerol droplets should be researched.

Recently, researchers have revealed that microexplosion occurs in binary fuel mixture droplets under specific temperatures when droplets consist of two liquids with different boiling point values. In addition, droplets fragment into smaller droplets violently at high temperatures since vaporization happens in interior of droplets driven by the high internal pressure and temperature inside each droplet. After microexplosion, secondary droplets are formed, which are all smaller than initial droplets. Because smaller droplets have higher surface-to-volume ratio, more complete combustion occurs resulting in greater power output. These phenomena also can lead to higher combustion efficiency, lower greenhouse gases and a reduction of NO_x emissions even when combusting glycerol-based mixtures.

In this research, microexplosion phenomena of methanol-in-glycerol mixtures have been studied using a high speed camera and an acoustic sensor system. A Fast Fourier Transform (FFT) algorithm has been used to analyze the collected data using Matlab to understand frequencies of microexplosion. In order to understand the effect of concentration of methanol in the droplets, three different concentrations of droplets were used under high temperature to induce microexplosion phenomena. Also the droplets were controlled at two sizes in order to study the effects of initial droplets size on microexplosion. Methanol was also replaced by water and mixed with glycerol to compare the results. Moreover, glycerol was selected in the study due to its unknown microexplosion potential.

The main goal of this study is to identify what conditions lead to the highest probability of microexplosion occurrence under certain temperatures, and to understand

the relationship between frequencies of microexplosion and droplet size. Methanol-in-glycerol mixtures with 5%, 10%, and 15% methanol were prepared and tested in a microexplosion chamber. Also, water-in-glycerol mixtures with 50% water were mixed and compared with the results of methanol-in-glycerol mixtures. Droplet sizes were controlled at 230 μm and 130 μm using nanoparticle based coatings to be able to understand the effect of discrete droplet size on microexplosion properties. Images of microexplosion were captured and acoustic emissions signals of microexplosion were detected at the same time since the high speed camera system and the acoustic sensor were synchronized using LabView. Finally, a FFT algorithm via Matlab was used to study microexplosion properties.

2. LITERATURE REVIEW

2.1 Past Research on the Studies of Microexplosion

Researchers have experimentally observed microexplosions in miscible fuel droplets and emulsified fuel droplets for many years. The phenomenon was first found by Ivanov and Nefdov [3] in 1965. Microexplosion occurs during droplet combustion since the droplets of miscible mixtures have two liquids with different boiling point values. As result of that, droplets fragment into smaller droplets violently at the high temperature. Furthermore, the less volatile and high boiling point liquid usually concentrates on the droplet's exterior. The droplet temperature can attain high values because of the low vapor pressure and high flash point of the mixture liquid with the highest boiling point. However, the droplet's interior consists of more volatile and low boiling point liquid, which tends to overheat reaching high pressure at high temperatures. This in turn leads to sudden bubble nucleation and sudden expansion or microexplosion caused by the high internal pressure of droplet. In summary, microexplosion is characterized by the formation of smaller droplets caused by a sudden expansion and rupture of droplets [4].

Three important properties of microexplosion have been studied [5]. First of all, microexplosion would occur when droplets consisting of two liquids with great difference in volatilities have the ideal mixture ratios. Studies have shown that an optimum amount of the less volatile liquid component should be identified so droplets can microexplode at high frequency. Furthermore, the concentration of the more volatile liquid component should be chosen carefully to ensure high temperature and bubble nucleation necessary

for effective microexplosion. Secondly, microexplosion is frequently characterized by homogenous bubble nucleation when the droplet surface temperature is very high. Finally, microexplosion occurs when the internal pressure of the droplet increases rapidly, which is driven by a substantial increase in temperature.

After microexplosion, secondary droplets are formed, which are all smaller than the initial droplets. Because smaller droplets have higher surface-to-volume ratio, more complete combustion occurs resulting in greater power output. In addition, the microexplosion of emulsified fuel of water and oil is advantageous in three ways: an increase in fuel efficiency, NO_x reduction and lower greenhouse gases (GHG) [6]. The fuel must be atomized into small droplets to ensure microexplosion. However, this burning is often incomplete since some larger droplets have insufficient time to combust. Because of microexplosion, secondary droplets have higher surface-to-volume ratio that help droplets burn completely. Moreover, water of droplets decrease the flame temperature leading to fewer emissions of NO_x. This is because NO_x is produced from the reaction of nitrogen and oxygen gases at high temperature. Furthermore, the addition of water increases OH radicals which is favorable to oxidize soot precursors [7]. It also decreases probability of pre-ignition and detonation occurrences in spark ignition engines [8]. Therefore, microexplosion leads to more complete combustion which increases engine efficiency and decreases air pollutions on a per mass basis.

Mikami et al. [9] studied the probability of microexplosion occurrence of miscible fuel mixtures. Droplets made of n-alkane (heptane, hexane, pentane and octane) and n-hexadecane mixture were injected into atmospheric air, where the initial droplet size was

controlled at 0.3 mm with about 10% uncertainty, and the injection pressure was set at 240 mm H_2O. In the experiments, fifty droplets were tested to obtain the probability of microexplosion occurrence. The highest probability of microexplosion was found when burning n-pentane/n-hexadecane droplets with 0.3 mole fraction n-hexadecane. Moreover, n-hexane/n-hexadecane droplets having 0.23 mole fraction n-hexadecane were tested with various droplet sizes. The probability of microexplosion increased from 5% to 85% when initial droplet size increased from 0.22 mm to 0.35 mm. The results indicate that at a certain concentration of high volatile liquids of droplets, the highest probability of occurrence in microexplosion can be found. Also, initial droplet size significantly affected the probability of microexplosion. The probability of microexplosion decreased when droplet size became smaller within a certain range.

Tsue et al. [10] conducted experiments to study microexplosion behavior of emulsion droplets. In the experiment, the droplets were made of base fuel (n-teteadecane or n-hexadecane), water and 1% surfactant. The water content varied from 10% to 30 % by volume. Also, single droplets were suspended at the tip of a quartz fiber. The initial droplet size was controlled at 1 mm. The authors found that the probability of microexplosion occurrence increased exponentially with an increase in water content. Watanabe et al. [11] also heated emulsified fuel, which was made of 10 % water, 89.25 % kerosene and 0.75 % surfactant, in order to understand the puffing and the microexplosion behavior. The results indicated that when the temperature of the furnace increased, the onset probability of puffing decreased. However, more microexplosion happened at higher furnace temperature.

Ferrante et al. [12] tested biofuel in a fluidized bed to observe microexplosion events. A video camera system and a pressure transducer were used to record the combustion process in the furnace. The temperature in the furnace was set from 600 °C to 700 °C to induce microexplosion phenomena. Also, each frame was analyzed to measure the luminosity index which represents the area of microexplosion. The pressure profile was recorded at 600 °C, 650 °C and 700 °C. Three figures showed that the pressure profiles became smoother with increasing temperature. They observed that the highest probability of microexplosion occurrence happened at 600 °C. Moreover, the author mentioned that there was no microexplosion at 800 °C and the pressure profile was observed to be very smooth.

Wang and Law [13] observed microexplosion phenomenon under different pressures. The water/oil emulsion droplets and miscible mixtures consisting of n-alkane (heptane, hexane, hexadecane and octadecane) and n-alcohol (butanol, dodecanol, ethanol, methanol and propane) were tested from 1 atm to 5 atm. Also, the ambient temperature was controlled from 1000 K to 1400 K. Microexplosion took place with specific concentrations of high volatile liquid in the droplets. The difference in volatilities between the two liquids also affected the occurrence of microexplosion. There was no microexplosion phenomenon in the experiment if the difference in volatility is not significant. Moreover, most of droplets showed that the normalized droplet size (d_e/d_o) increased with increasing pressure. Finally, higher environment pressure leads to higher probability of microexplosion.

Hsieh et al. [14] experimentally investigated microexplosion of water-in-oil compound droplets without using surfactant. In their experiments, tiny water droplets were was suspended on the thermocouple next to hexadecane droplets, which led to the formation of a binary droplet within the microexplosion chamber. The heating environment was controlled at 320 °C, 400 °C and 500 °C. Also, a high speed camera was used to record the behavior of microexplosion. Based on observations, microexplosion can be classified in three modes: direct explosion, partial explosion and swelling. The direct explosion unusually takes place at 400 °C and 500 °C. However, partial explosion and swelling only occurred at 320 °C. Also, it took longer time when direct explosion occurred. The results indicated that temperature affected the strength of microexplosion. This is because at higher temperature, the rate of nucleation increases drastically leading to violent microexplosion.

2.2 Acoustic Emission

Acoustic emission (AE) is a phenomenon defined as the spontaneously rapid released energy of stressed materials [15]. Since all materials have certain elasticity, they release elastic energy after being compressed or strained under different forces. Also, ideal sensors can detect those elastic waves on the surface of materials. Those data can be analyzed to measure the frequencies associated with rapid expansion.

AE testing is also considered as non-destructive testing method [15]. The advantage of this method is that it can be applied under working loads. However, other non-destructive testing methods are applied before or after working loads. The

applications of AE testing are in many areas such as seismic research, material research, and inspection. In other words, it can be used to observe damage, monitor welding processes, detect fatigue failures, and observe leakages of tanks [16].

2.2.1 Acoustic Emission Testing Equipment

Acoustic Emission Sensors

An acoustic emission sensor is also called a transducer because it converts energy of elastic waves into electrical signals [17]. In addition, piezoelectric transducer have been most commonly used in AE testing due to high sensitivity and ruggedness. The piezoelectric transducer is made of small crystal mixture of Titanates and Zirconates mixed with other materials. The surface of piezoelectric ceramics is metalized to pass electricity [17]. Figure 1 shows the setup of an AE sensor.

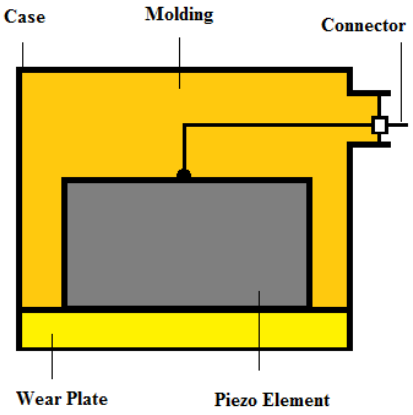

Figure 1. Basic setup pf an AE sensor [16].

To minimize the loss of mechanical energy, a piezoelectric transducer should contact the flat surface of material so that the sensitivity of AE sensor could be larger. Also, when AE sensor contacts flat surface, using some oil, grease or epoxy adhesive can assure there is no air to affect the transmission of shear waves between them. That is a very important step for acoustic sensor to detect signals clearly.

Preamplifier

The function of the preamplifier is to obtain high sensitivity by magnifying the initial electrical signal coming from AE sensor without enormously degrading the signal-to-noise (SNR). The definition of SNR is the ratio of signal strength to background noise strength which can be written as follows:

$$dB = 20\log\left(\frac{V_{signal}}{V_{noise}}\right) \tag{1}$$

Preamplifiers usually offer 20 dB, 40 dB and 60 dB gain ranges, and the initial electrical signals are magnified ten times, a hundred times and a thousand times, respectively.

2.3 Signal Processing

Signal processing includes analog signal processing, discrete time signal processing, digital signal processing and nonlinear signal processing. Analog signal

processing (ASP) is used to represent signals mathematically before they are digitized. In digital signal processing (DSP), discrete time signals are digitized by an analog-to-digital converter (ADC) [18]. In addition, there are three major types of digital signal processing, including time domain, space domain, frequency domain and wavelet domain. Time domain is characterized by waves described by their amplitudes as a function of time. In the case of space domain, multiple variable signals can be processed. Frequency domain comes from time and space domain by using Fourier transform.

The most important part in digital signal processing is the sampling rate, also called sampling frequency, which is the reduction of a continuous signal to a discrete signal. The definition of sampling frequency (f_s) is the number of samples that can be obtained per second. The following equation (2) shows the relationship between the sampling frequency and the sampling interval (*T*).

$$f_s = \frac{1}{T} \tag{2}$$

The Nyquist-Shannon sampling theorem should be considered when analog signals are converted to digital signals. The theorem indicates that the sampling frequency must be greater than two times the highest frequency of the original signal [18]. The lower sampling frequency leads to aliasing which makes the result not distinguishable.

2.3.1 Fast Fourier Transform

Fast Fourier transform (FFT) is an efficient method to compute the Discrete Fourier Transform (DFT) of data samples [19]. Discrete Fourier transform is one of Fourier transform, which is a mathematical algorithm used to convert the function from time domain to frequency domain. The Discrete Fourier Transform of the discrete Fourier series *x(r)*, r = 0, 1, 2… (N – 1) is defined as follows:

$$X_k = \frac{1}{N}\sum_{r=0}^{N-1} x_r e^{-i(2\pi kr/N)} \tag{3}$$

where, $k = 0, 1, 2\ldots (N-1)$

Equation (3) can be solved directly or by using Fast Fourier Transform. When solving the equation directly, it requires N^2 multiplications to evaluate X_k. This is because it should evaluate N multiplications of X_k for each of N. However, it can be reduced by an order $N\log_2 N$ when using Fast Fourier Transform approach. For the case of $N = 2^{10}$, using the direct approach would require more than 100 times computing than using Fast Fourier Transform. Therefore, the Fast Fourier Transform approach not only reduces computation time but also increases accuracy essentially [19].

2.4 Pencil Lead Break Test

Hsu-Nielsen source [20], which is also called the pencil lead break, is a test to simulate acoustic emission signals. The test is performed by breaking a graphite lead as

shown in Figure 2. A graphite lead, which is about 2 mm long and 0.5 mm (or 0.3 mm) in diameter, is broken by hitting it on a hard surface. This action generates a strong acoustic emission signal for many purposes. Firstly, it assures that the transducer works perfectly before conducting any acoustic experiments. Secondly, it can be used to accurately determine the location of the acoustic source. Finally, the velocity of an acoustic wave can be calculated from this test.

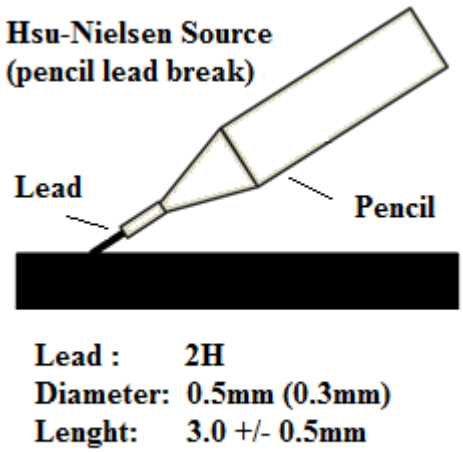

Figure 2. Schematic of pencil lead break [20].

Yu et al. [21] performed pencil lead break tests before and after each loading to ensure the workability of the transducer. Also, the test was performed in order to obtain the reference acoustic emission waveforms, which are routinely referred as friction emission. Vallen [16] also used pencil break lead test to measure the thickness and hardness of vessels, as well as to check the performance of sensors.

2.5 Past Research on the Microexplosion Detection by Acoustic Sensors

Yamasaki et al. [22] used a high speed camera system and an acoustic emission sensor system to study microexplosion phenomena. They used a single droplet emulsion made of 20% of n-hexadecane and 80% of water, which was burned at the tip of a quartz fiber stick to observe internal boiling and microexplosion. In their study, the sampling frequency of the acoustic emission sensor was set at 0.2 MHz. From the high speed camera system, images of puffing and microexplosion phenomena were captured. Acoustic emission signals of a n-hexadecane/water emulsion droplet were detected by the acoustic sensor system as shown in Figure 3.

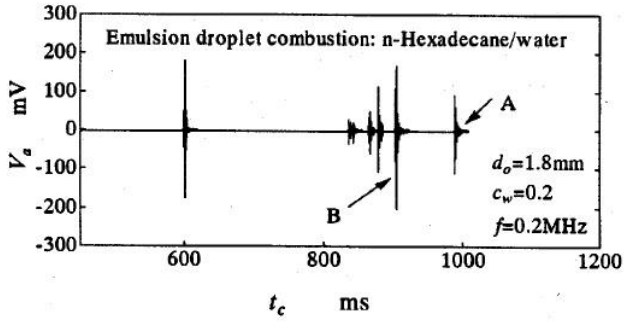

Figure 3. Acoustic emission signals of a n-hexadecane/water emulsion droplet [22].

From Figure 3, higher amplitude indicates puffing (point B) and microexplosion (point A) occurrence. Some signals were detected before microexplosion since internal boiling and puffing also happened during the heating process. After microexplosion, the acoustic sensor could not detect any significant acoustic signals. In addition, there was no microexplosion under the same temperature if pure n-hexadecane was used as fuel.

Tanaka et al. [23] conducted experiments to study microexplosion and its acoustic emission using a high speed camera system and a microphone system. Two types of droplets, which were made of 70% n-tetradecane with 30% water, and 80% n-hexadecane with 20% water, were tested in their experiments. Also, a Birchley-Riley [10] composite droplet and a W/O emulsion droplet were tested to understand the effect of composition on microexplosion results.

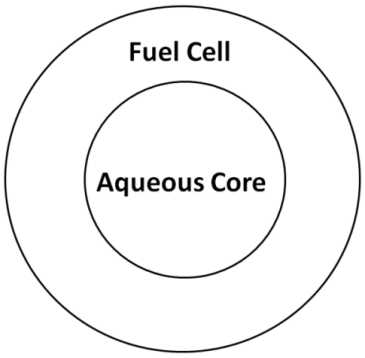

Figure 4. Fuel droplet of Birchley-Riley model [23].

The interior of Birchley-Riley fuel droplet consists of water surrounded by a fuel liquid. Microexplosion phenomena happened when W/O emulsion droplets or B-R fuel droplets were exposed to high temperatures. Also, the microexplosion acoustic wave was detected by a microphone. However, puffing events could not be detected by using a microphone due to its limited sensitivity of microphone. The authors also used the Fast Fourier Transform to analyze acoustic signal data to determine the signal properties including the corresponding frequencies. The frequency spectrum of puffing indicated

high sound pressure level from 0 to 2 kHz, but the frequency spectrum of microexplosion showed high sound pressure level from 0 to 20 kHz.

Nam [24] conducted experiment to observe microexplosion of methanol-in-canola and water-in-canola emulsified blend by using a high speed camera system and an acoustic emission sensor system. The effects of temperature, droplet size and composition on microexplosion were studied. In addition, the acoustic waves of microexplosion were detected and used to determine the characteristic frequencies of the phenomena. The results showed that higher concentration of methanol and water caused higher probability of microexplosion. Furthermore, higher temperature led to lower probability of puffing event due to more complete evaporation and microexplosion. Results obtained by Nam [24] showed that the size of secondary droplets depended on initial droplet size. Larger initial droplet size had larger secondary droplet size due to surface tension effects. Finally, droplet sizes also affected frequencies of microexplosion. Smaller droplet size of droplet led to broader frequencies. In other words, higher frequencies were detected when smaller droplets microexploded.

Despite recent studies in the area of microexplosion of fuel droplets, little is known how droplets made of two homogeneous fuels might microexplode under controlled conditions. The effects of fuel composition and droplet size on microexplosion should be explored in greater detail.

3. RESEARCH OBJECTIVES

The main goal of this study is to determine the fuel conditions that lead to the highest probability of microexplosion occurrence under certain ambient conditions. Furthermore, it seeks to understand the relationship between frequencies of microexplosion and droplet properties and ambient conditions. A high speed camera system was used to observe microexplosion processes, and an acoustic emission sensor system was used to detect acoustic waves of microexplosion. In order to meet all the stated objectives, the following tasks were undertaken and completed.

a. Prepare methanol/glycerol and water/glycerol mixtures as depicted in Table 1.

Table 1. Composition of mixtures

Abbreviated Name	Full Name	Base Fluid	Secondary Fluid
GM 95/5	Methanol-in-glycerol	95 % Glycerol	5% Methanol
GM 90/10	Methanol-in-glycerol	90 % Glycerol	10% Methanol
GM 85/15	Methanol-in-glycerol	85 % Glycerol	15% Methanol
GW 50/50	Water-in-glycerol	50 % Glycerol	50 % Water

b. Measure the contact angle of mixture droplets on different surfaces with different coatings.

c. Make and control droplet size using coated platinum wire. Droplet sizes were 230 μm and 130 μm using bare and nanoparticle-coated surfaces, respectively.

d. Determine the highest probability of microexplosion occurrence at certain temperatures and droplet properties as stipulated in Table 2.

Table 2. Input variables

Mixtures Type	Droplet Sizes
GM 95/5	230 μm 130 μm
GM 90/10	
GM 85/15	
GW 50/50	

e. Detect and characterize the frequency of microexplosion at the temperature when the highest probability of microexplosion occurs.

f. Formulate a relationship between droplet properties and the microexplosion acoustic response.

4. EXPERIMENTAL SETUP

An experimental setup was designed and assembled to record images of microexplosion and to detect microexplosion wave signals. LabView and Matlab were used to record and analyze the acoustic emission signals imaged and sensed by a high speed camera and acoustic sensor, respectively. Figure 5 and 6 show the overall experimental setup, which was based on Yamasaki's experimental system [22]. The following subsections describe each subsystem in detail.

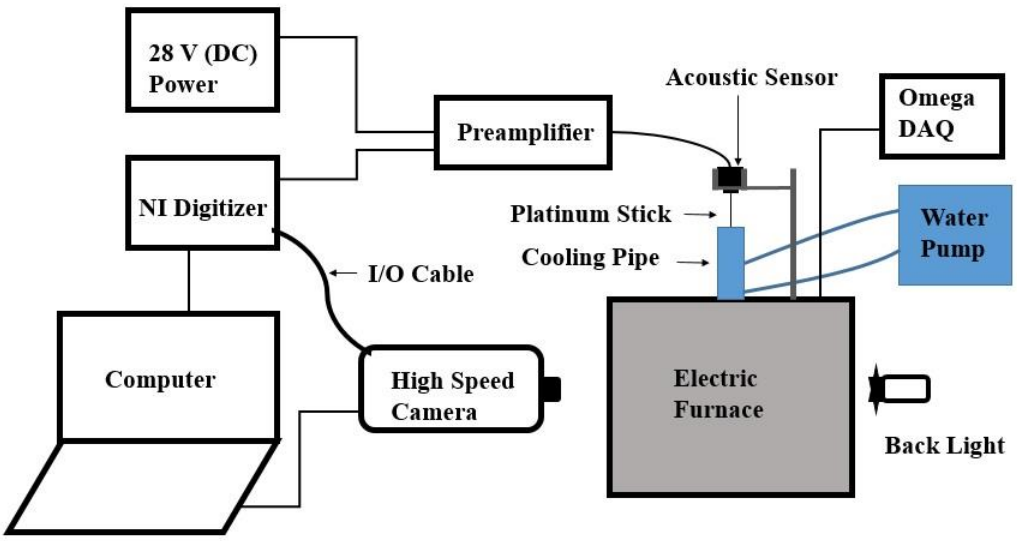

Figure 5. Experimental setup.

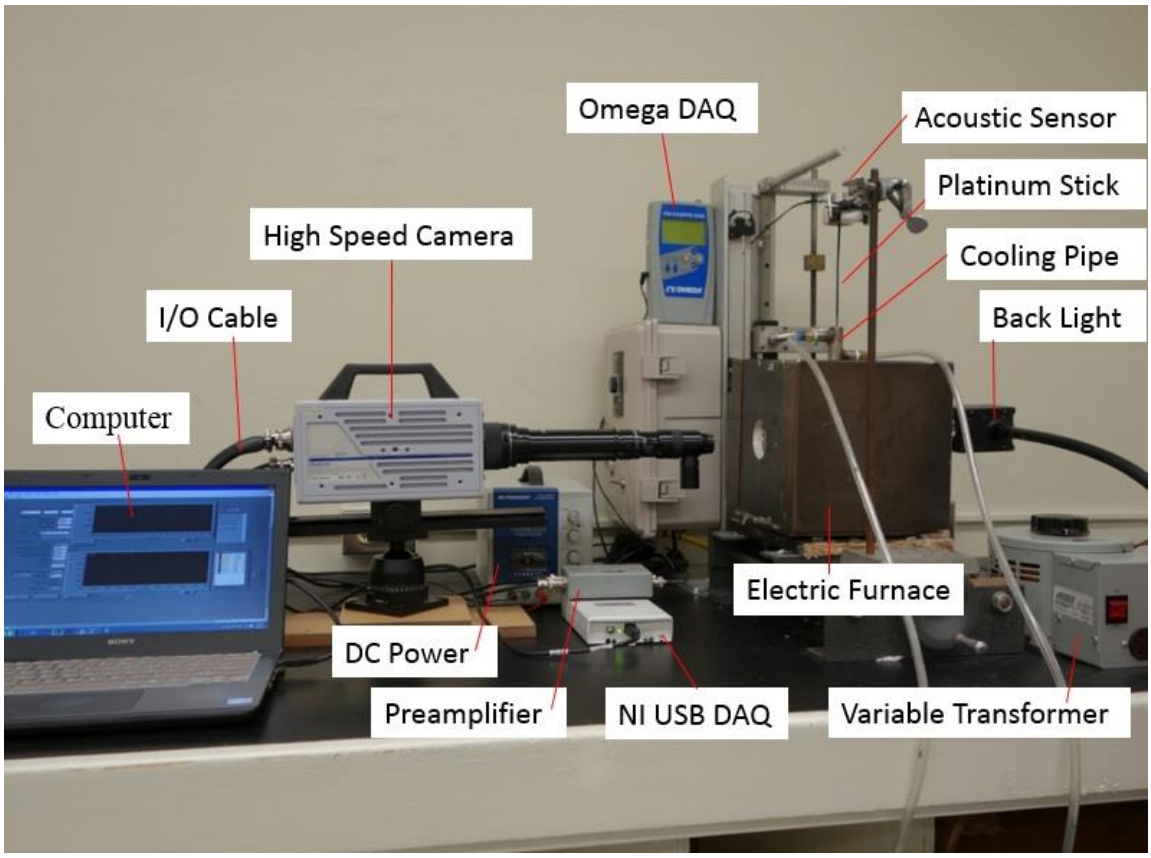

Figure 6. Experimental setup.

4.1 High Speed Camera System

A high speed camera system, FASTCAM SA3, was purchased from Photron. It was used to record images with a 0.5X magnification lens to observe the microexplosion phenomena. The high speed camera can record 1000 images per second with a resolution of 1024 x 1024 pixels, and up to 60,000 images per second with a resolution of 128 x 16 pixels. In addition, Photron FASTCAM viewer is a software used to control the high speed camera system using a computer. Many icons such as frame rate, resolution, and shutter speed can be set via the software.

An I/O port cable was purchased from Digital West Imaging. A fiber optic cable was used to synchronize the high speed camera system with the acoustic emission system. One side of the cable was connected to the high speed camera, while the other side (General In port) was connected to the Programmable Function Interface (PFI) port of the National Instrument USB digitizer.

4.2 Acoustic Emission Sensor System

An acoustic emission sensor system was used to detect acoustic signals caused by microexplosion phenomena. A platinum stick was attached to the acoustic emission sensor to transmit microexplosion waves. The waves travelled through 2/4/6 Preamplifier to the National Instrument USB digitizer, which collected all the data. Figure 7 shows the setup of the acoustic emission sensor system.

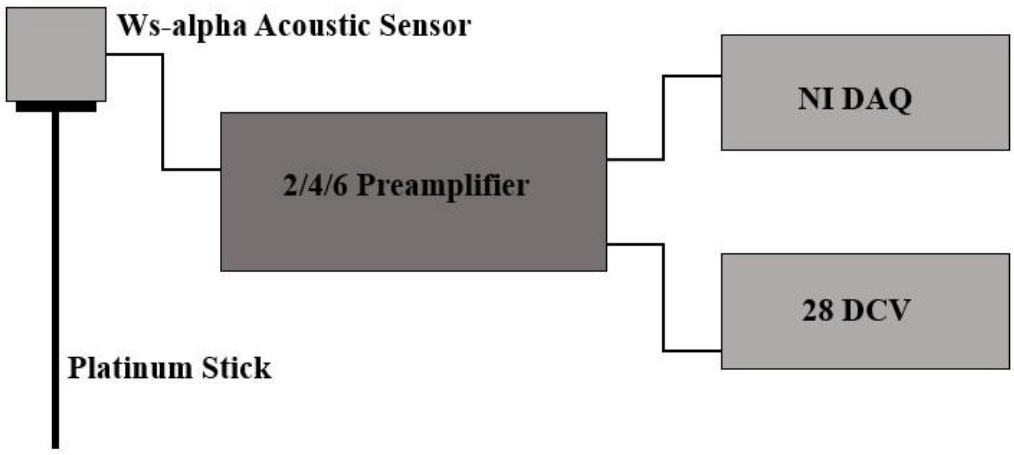

Figure 7. Acoustic Emission Sensor System.

4.2.1 Platinum Stick

A platinum Stick with a diameter of 1 mm was used to transmit acoustic waves generated by the microexplosion of droplets to the National Instrument USB digitizer. Platinum Wire with a diameter of 25.4 μm purchased from A-M Systems was attached to the tip of the platinum stick by using a high-temperature ceramic adhesive. The platinum wire was used to suspend a micro-sized droplet during droplet expansion and microexplosion processes. The platinum stick and platinum wire were selected due to their high melting point of 1768.3 °C. In addition, a 10 mm diameter circular plate was attached to the other tip of Platinum Stick to be able to contact the Ws-alpha acoustic emission sensor as shown in Figure 8.

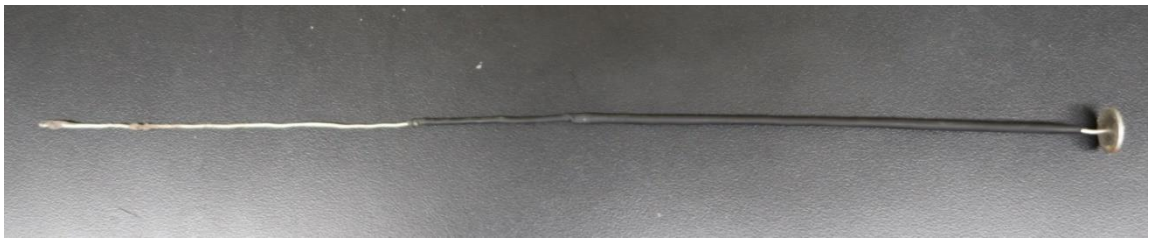

Figure 8. Platinum Stick.

4.2.2 Ws-alpha Acoustic Emission Sensor and 2/4/6 Preamplifier

The acoustic emission sensor, Ws-alpha, was purchased from Mistras, USA. It is a single-ended and wideband frequency acoustic emission sensor, and the operating frequency reaches up to 1.0 MHz. The 2/4/6 preamplifier was used to magnify the power of the acoustic signals by 20 dB, 40 dB and 60 dB. It was connected to the acoustic emission sensor to receive the acoustic signals. Also, the preamplifier was powered by

28V of DC variable transformer. The Ws-alpha acoustic emission sensor and 2/4/6 preamplifier are shown in Figure 9.

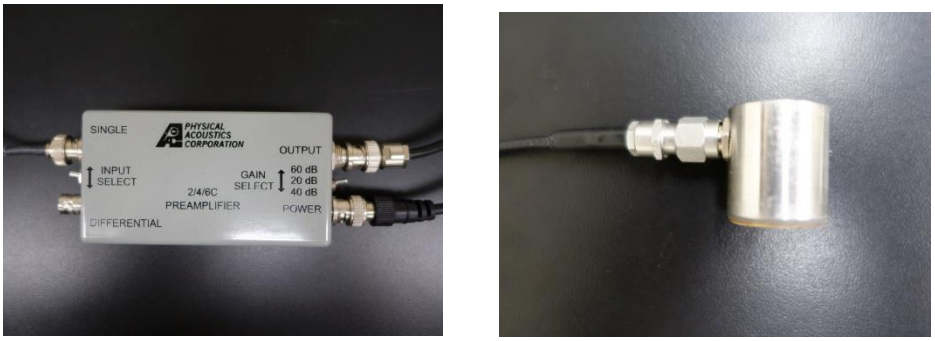

(a) (b)

Figure 9. (a) 2/4/6 preamplifier and (b) WS-alpha acoustic emission sensor.

4.2.3 National Instrument USB Digitizer

A National Instrument Data Acquisition digitizer, USB-5132, was used to receive acoustic signal data. It is very portable and convenient for users because it comes with a USB port. The eight-bit digitizer features 50 MS/s sampling rates on two simultaneously sampled channels. It comes with an 8 MB of onboard memory to capture the data. Also, the PFI port of the digitizer was connected to the I/O cable to synchronize the high speed camera. The NI USB-5132 digitizer is shown in Figure 10.

Figure 10. National Instrument USB-5132.

4.2.4 LabView Coding

A LabView code was written using the niScope library for the National Instrument USB-5132 digitizer. Figure 11 shows the front panel LabView window on a personal computer. An input parameter control box, which can control the whole acoustic emission sensor system, is shown on the left. Also, the acoustic wave signal and the frequency spectrum are shown on the right. The sampling rate was set at 1 MHz, resulting in 3,000,000 recordings in 3 minutes. An edge trigger option was set at 200 mV to start recording acoustic signals.

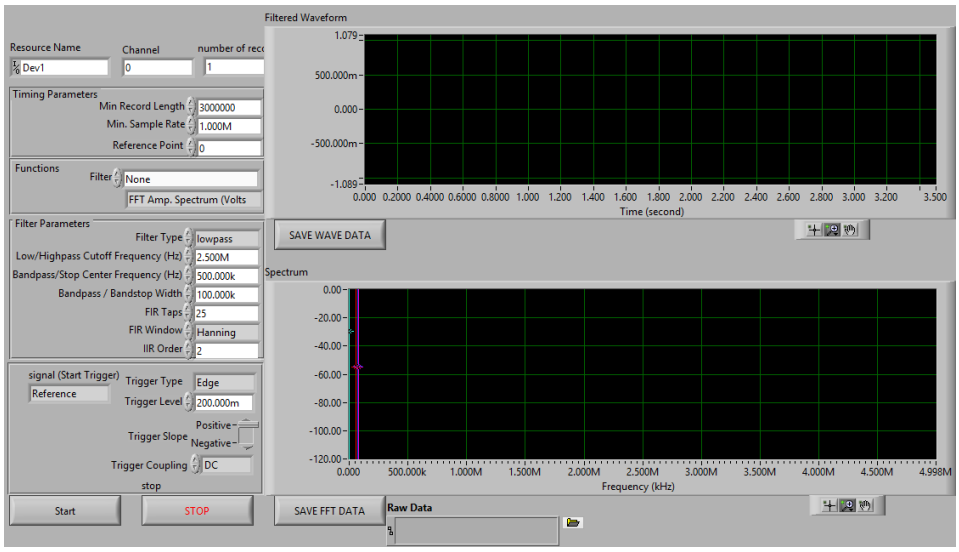

Figure 11. LabView front panel.

4.3 System Synchronization

In order to ensure high speed camera images match the corresponding acoustic signals, a pencil lead break test was performed the experiments. After synchronization of the two systems, the high speed camera system and the acoustic emission sensor system recorded data simultaneously. Figure 12 shows when a pencil lead strikes on an iron plate as recorded by the high speed camera system, which was triggered by LabView. Figure 13 shows the acoustic response during the lead pencil test. As both figures show, the pencil lead strike also was recorded by the high speed camera system and the acoustic emission sensor system simultaneously. This test confirmed that the two systems were synchronized successfully.

(a)	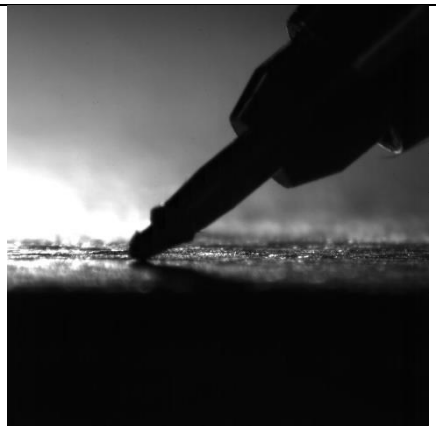	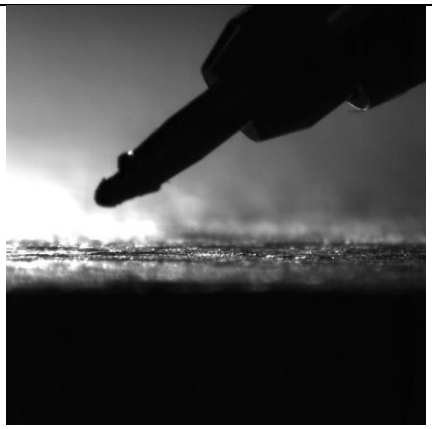
	0 seconds	1.25 seconds
(b)		
	0.903 seconds	0.904 seconds

Figure 12. Images of pencil lead break test (a) first strike (b) second strike.

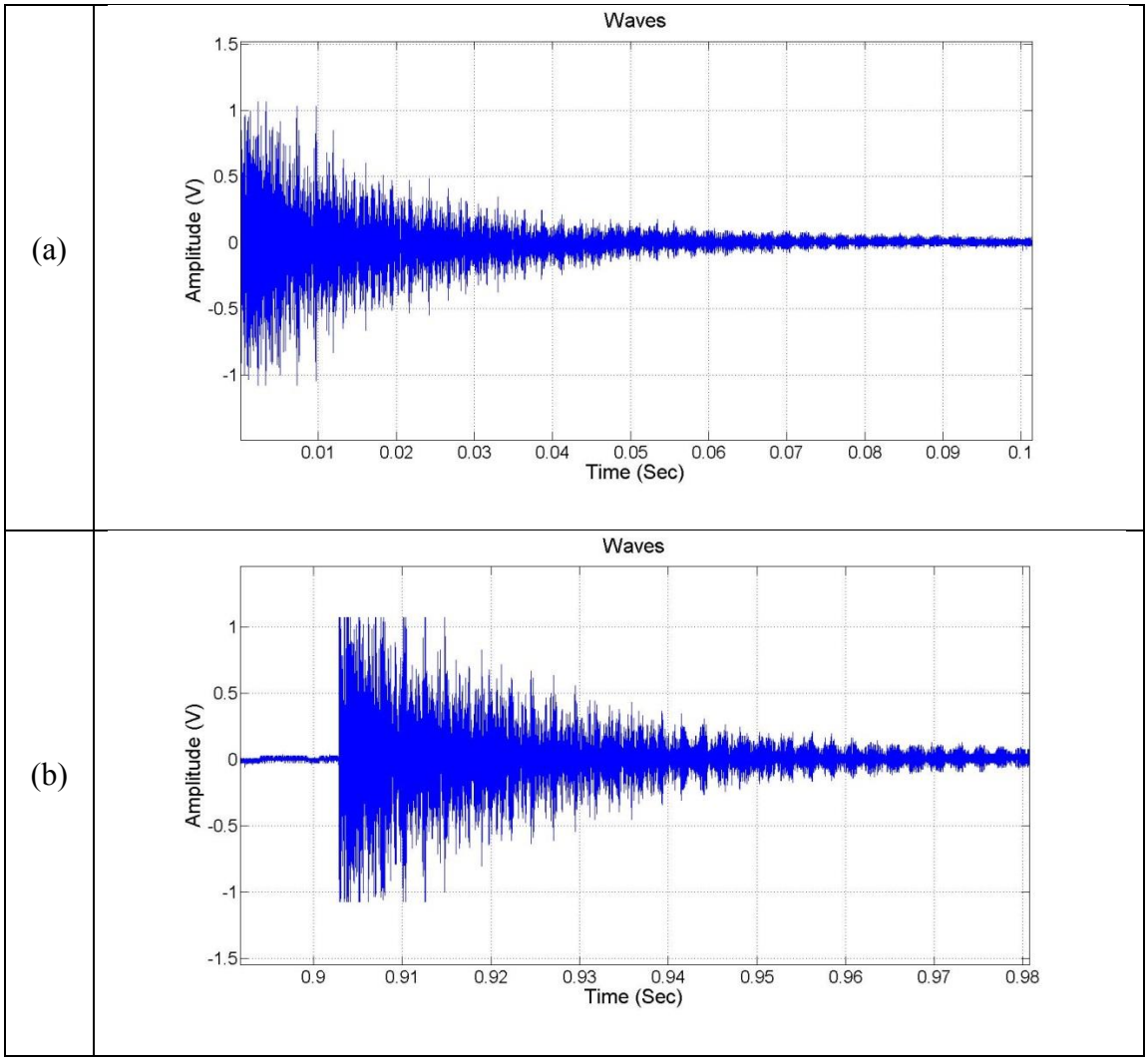

Figure 13. Waveform of synchronization test (a) first strike (b) second strike.

4.4 Electric Furnace

A cubic electric furnace was made from two cover iron plates and four flat iron plates to provide a high temperature environment necessary to promote microexplosion of emulsified mixtures. The dimensions of two cover iron plates were 220 mm × 215 mm × 40 mm, and four flat iron plates were 210 mm × 205 mm. The thickness of the iron plates

were 2 mm. A high speed camera and backlight used two 53 mm glass covered holes, which were on the center of two flat plates, to record images inside the furnace. Two extreme temperature quartz pure glasses were used as windows. Also, a 28 mm hole, which was on the center of the flat plate, was used to insert the water pipe and the platinum stick inside the furnace. Furthermore, one of cover iron plates had a 1 mm hole used to insert a K-type thermocouple in the furnace to record the ambient temperature. Inside the furnace, high temperature cement was used as insulation material within the furnace. The 20 mm thickness of high temperature cement was used to insulate the chamber. Electric heating wires were placed on the ceramic insulation fiber, which were attached to the high temperature cement, around the chamber in order to provide uniform heating.

4.5 Cooling Pipe

The outer of cooling pipe was made of inconel that can endure up to 1300 °C. The inner of cooling pipe was made of iron. The external diameter of cooling pipe was 18 mm while the internal one was 7 mm in diameter. The cooling pipe was used for two main reasons. Firstly, the cooling pipe was used to provide more time for the high speed camera system to record images before the droplet experienced microexplosion. The cooling pipe prevented each droplet from being exposed immediately to excessive heat within the chamber. Secondly, the noise generated by the vertical motion of the cooling pipe upon retrieval was used to activate the acoustic sensor system and high speed camera simultaneously. Figure 14 shows graphically the purpose of the cooling pipe.

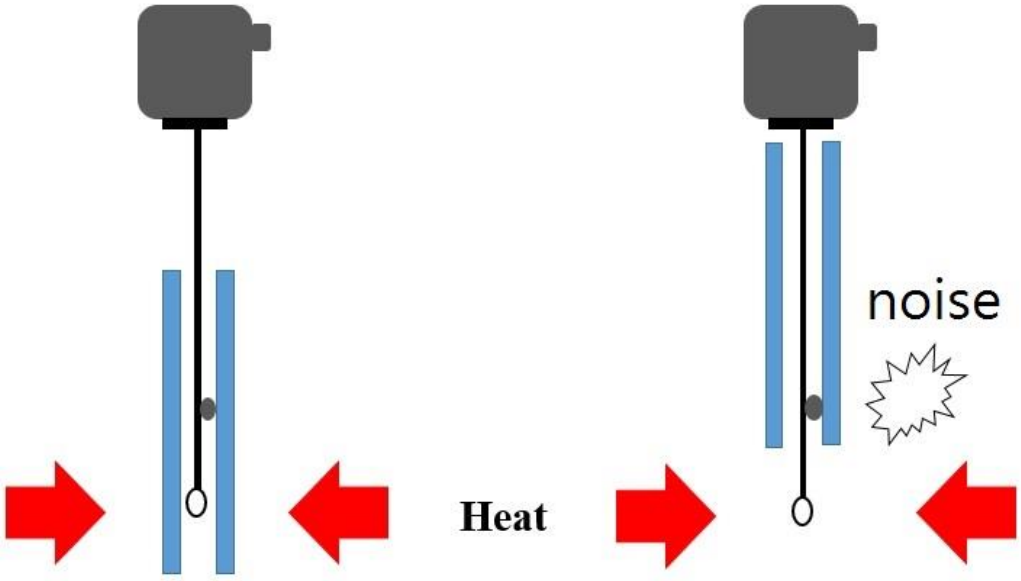

Figure 14. Purpose of cooling pipe.

4.6 Temperature Measurements

A type K thermocouple was connected to the Omega DAQPRO-5300 in order to monitor the temperature inside the electric furnace. Also, the Omega DAQPRO-5300 recorded temperature data every second during the experiments.

4.7 Mixtures Preparation

In this experiment, methanol-in-glycerol and water-in-glycerol mixtures were made to understand the effect of methanol and water concentration on the occurrence of microexplosion phenomena at high temperatures. 99.5 % concentrated glycerol from MACRON, 99.98 % concentrated methanol from VWR, and distilled water were used to make the fuel mixtures. Table 3 shows the properties of all liquids used in the experiment. Four fuel mixtures were prepared as shown in Table 4.

Table 3. Properties of all liquids

Chemical and Physical Properties	Glycerol	Water	Methanol
Molecular Formula	$C_3H_8O_3$	H_2O	CH_4O
Boiling Point [˚C]	290	100	65
Vapor Pressure [kPa] at 25˚C	0.00001	3.17	16.9
Surface Tension [dyne/cm]	63.2	72.75	22.95

Table 4. Mixtures information on weight basis

Abbreviated Name	Full Name	Base Fluid	Secondary Fluid
GM 95/5	Methanol-in-Glycerol	95 % Glycerol	5% Methanol
GM 90/10	Methanol-in-Glycerol	90 % Glycerol	10% Methanol
GM 85/15	Methanol-in-Glycerol	85 % Glycerol	15% Methanol
GW 50/50	Water-in-Glycerol	50 % Glycerol	50 % Water

4.8 Droplet Size Measurement

Droplet sizes were measured from images captured using the high speed camera system. The resolution of images was 3.94 μm/pixel in the experiments. As seen in Figure 15, a droplet size was determined by counting the number of pixels within a droplet along the x-axis and the z-axis. Because the droplet was ellipsoidal, the length of the droplet along the y-axis was assumed to be the same as the length along the z-axis based on the principle of continuity. Therefore, the volume of the droplet was calculated using Equation (4). In order to simplify the calculation, all droplets were regarded as spherical. Finally, the radius of the droplet was obtained using Equation (5).

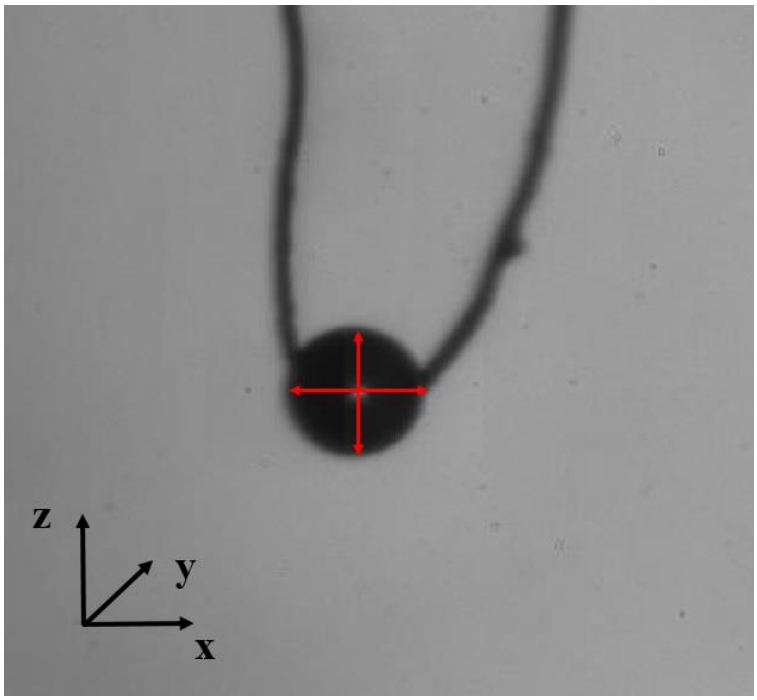

Figure 15. Droplet size measurement.

$$V_{ellipse} = \frac{4}{3}\pi\left(r_x \cdot r_y \cdot r_z\right) \tag{4}$$

where, $r_y = r_z$

$$r_{sphere} = \left(\frac{3 \cdot V_{ellipse}}{4\pi}\right)^{1/3} \tag{5}$$

4.9 Oleophobic Coating of the Acoustic Sensor Platinum Wire

In order to make droplet smaller on a platinum wire, the surface of the platinum wire was coated using Aculon-E to make the surface oleophobic. Aculon-E is an oleophobic surface treatment, which is easy to apply. The thickness of the applied coating

treatment was very thin, but it was durable. Before the coating was applied, Aculon 905, which is a water-based cleaner, was used to clean the surface. It was used to remove a variety of contaminants from the surface. Specifications about Aculon- E and Aculon 905 can be found in the appendix.

A platinum foil purchased from SIGMA-ALDRICH was used to measure droplet contact angle on a platinum surface. The dimension of platinum foil was 25 mm × 25 mm × 0.025 mm, as shown in Figure 16.

Figure 16. Platinum foil.

The following was the procedure [25] [26] used for coating oleophobic treatments on a Platinum foil:

1. Degrease all metal surface with methanol.
2. Dip the platinum foil in Aculon 905 cleaner for five minutes.
3. Hold the cleaned platinum foil under running distilled water for one minute.
4. Immerse the platinum foil in Aculon-E for one minute.

5. Air dry at room temperature.

Figure 17 shows droplets of water and different mixtures on the platinum foil surface. The contact angle of droplets increased after the platinum foil surface was coated by using Aculon-E. Table 5 shows the contact angles of droplets on a platinum foil surface.

(a)	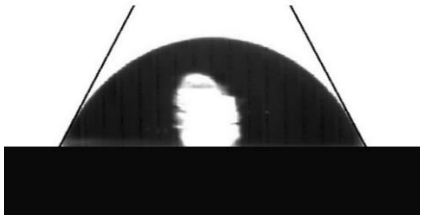	
b)	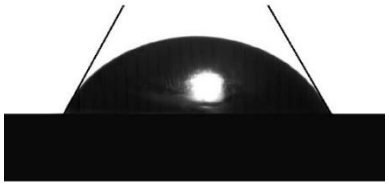	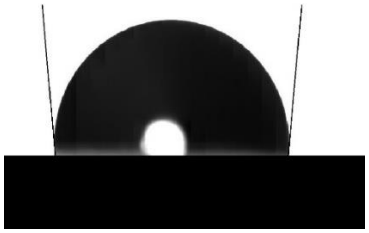
c)	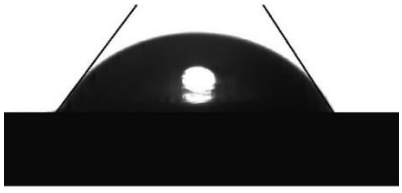	
	Before coating on platinum foil	After coating on platinum foil

Figure 17. Droplets on a platinum foil (a) water (b) GM 95/5 (c) GM 90/10 (d) GM 85/15 (e) GW 50/50.

(d)	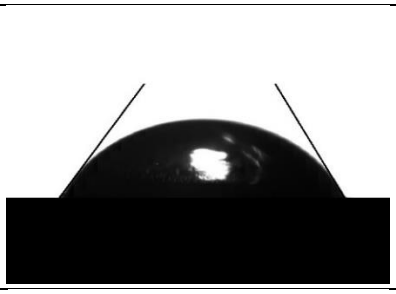	
(e)	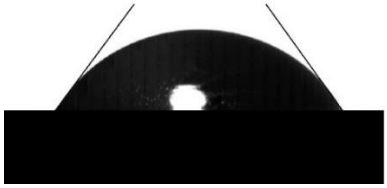	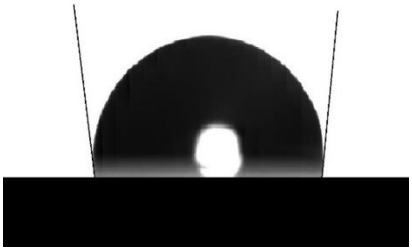
	Before coating on platinum foil	After coating on platinum foil

Figure 17. Continued.

Table 5. Contact angle of droplets on platinum foil

Droplets Type	**Droplet contact angle on original platinum foil**	**Droplet contact angle on coated platinum foil**
Water	62.0°	105.7°
GM 95/5	60.4°	96.1°
GM 90/10	59.9°	90.3°
GM 85/15	59.9°	87.4°
GW 50/50	57.9°	96.9°

The procedure used for coating oleophobic treatments on a platinum wire was the same as the procedure for a platinum foil. The results shown in Table 5 show that smaller droplets could be made on the platinum wire if coated with an oleophobic coating. Table 6 shows droplet sizes on the uncoated and coated platinum wires.

Table 6. Smallest droplet size on a platinum wire

Droplets Type	**Smallest droplet size on an original (uncoated) Platinum wire (μm)**	**Smallest droplet size on a coated Platinum wire (μm)**
GM 95/5	174 ± 8	120 ± 6
GM 90/10	181 ± 5	129 ± 5
GM 85/15	178 ± 8	123 ± 3
GW 50/50	187 ± 6	123 ± 6

5. RESULTS AND DISCUSSION

This chapter includes the probability of microexplosion occurrence and the signal analysis of microexplosion. Methanol-in-glycerol and water-in-glycerol mixture droplets were tested in order to determine the effects of concentration of secondary fluid and initial droplet size on microexplosion phenomena. All the results are discussed in detail in the following subsections.

5.1 Probability of Microexplosion Occurrence

The first goal of this research was to identify the conditions that lead to the highest probability of microexplosion occurrence at certain temperatures. In this part, images obtained using the high speed camera system, were used to identify microexplosion phenomena. In addition, ten identical droplets were tested at a single temperature in order to determine the probability of micorexplosion occurrence.

In general, microexplosion phenomenon takes place when a binary fuel mixture droplet fragments into smaller droplets violently at high temperatures. A microexploded droplet is driven by the high internal pressure inside the droplet. Figure 18 shows a microexplosion event of GM 90/10 mixture, which took place in less than 1 ms.

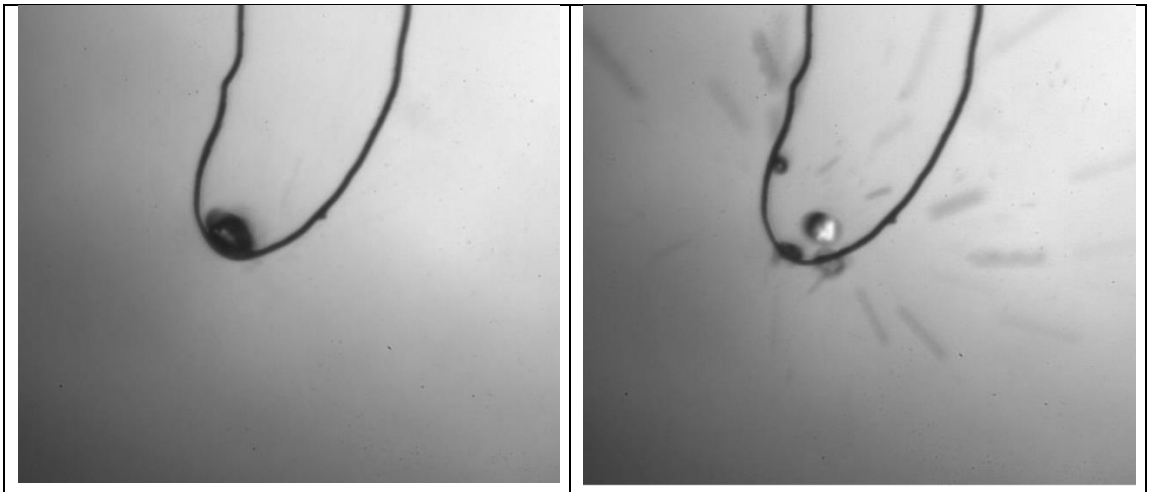

(a) 0.436 seconds | (b) 0.437 seconds

Figure 18. Microexplosion event of GM 90/10 mixture

5.1.1 Methanol-in-Glycerol Mixtures

Probability of Microexplosion Occurrence of Glycerol-in-Methanol Mixtures

In order to find what conditions lead to the highest probability of microexplosion occurrence of glycerol-in-methanol mixtures, glycerol-in-methanol mixtures with 5%, 10%, and 15% methanol were tested. Also, initial droplet sizes were controlled at 230 μm and 130 μm using nanoparticle based coating. Ten identical droplets were heated in the furnace at a single temperature. Therefore, the probability of microexplosion occurrence could be obtained by using statistical analysis.

The probability of microexplosion occurrence of GM 95/5 mixtures is shown in Figure 19. The average initial droplet size was 222 μm with a standard deviation of 8 μm. The highest probability of microexplosion occurrence was 70% at 680 ℃. Also, the

probability of microexplosion occurrence was 50% when temperatures were 650 ℃ and 710 ℃.

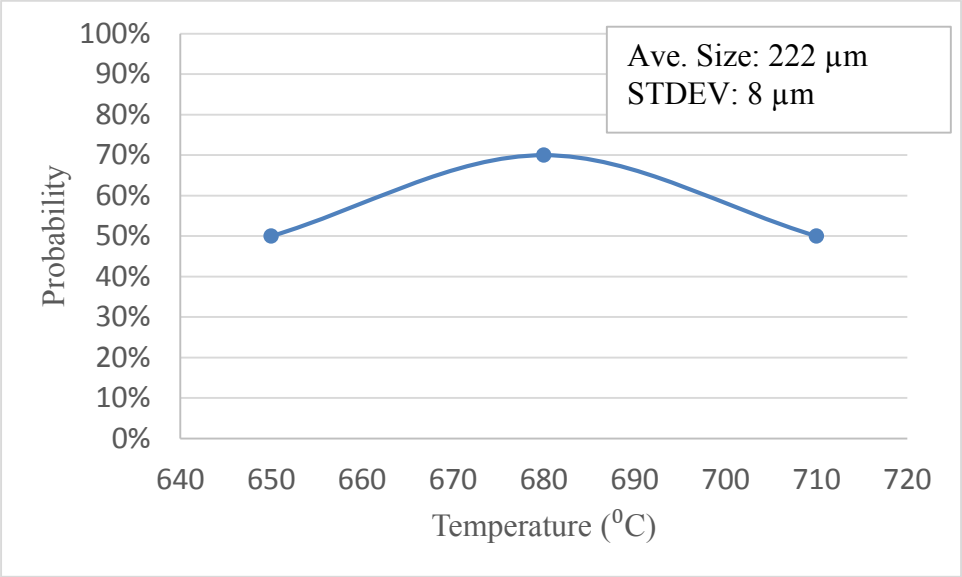

Figure 19. Probability of microexplosion of GM 95/5 mixtures with 222 µm of initial droplet size.

The probability of microexplosion occurrence of GM 95/5 mixtures with smaller droplets is shown in Figure 20. The average initial droplet size was 136 µm with a standard deviation of 9 µm. The highest probability of microexplosion occurrence was 40% at 530 °C because of the small sizes of the droplets. Also, the probability of microexplosion occurrence was 20% when temperatures were 500 ℃ and 560 ℃.

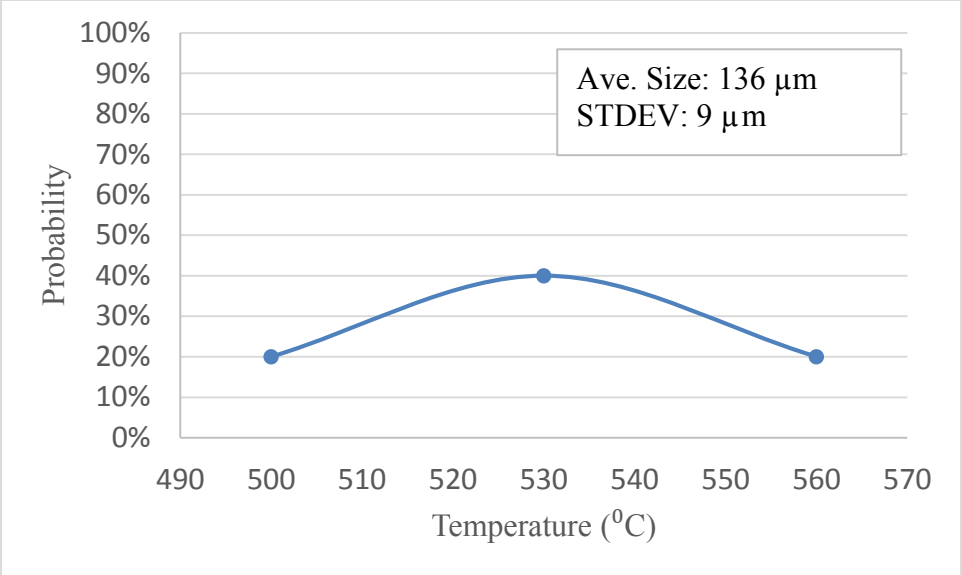

Figure 20. Probability of microexplosion of GM 95/5 mixtures with 136 µm of initial droplet size.

Next, the concentration of methanol in the methanol-in-glycerol mixture droplets was increased from 5% to 10%. The probability of microexplosion occurrence of GM 90/10 mixtures is shown in Figure 21. The average initial droplet size was 223 µm with a standard deviation of 11 µm. The highest probability of microexplosion occurrence increased to 90% at 680 ℃. Also, the probabilities of microexplosion occurrence were 50%, 70%, and 50% when temperatures were 600 ℃, 650 ℃, and 710 ℃, respectively.

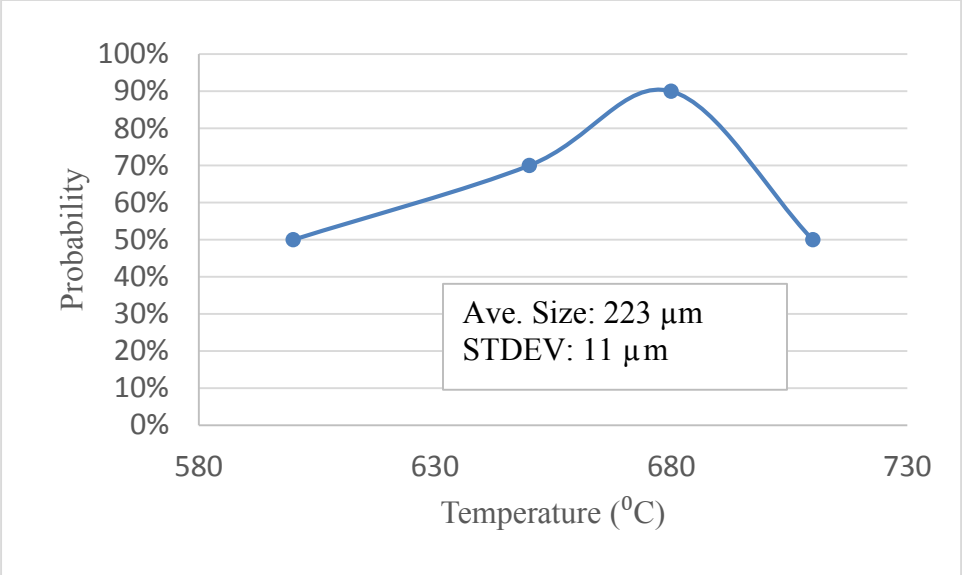

Figure 21. Probability of microexplosion of GM 90/10 mixtures with 223 µm of initial droplet size.

The probability of microexplosion occurrence of GM 90/10 mixtures with smaller droplets is shown in Figure 22. The average initial droplet size was 134 µm with a standard deviation of 9 µm. The highest probability of microexplosion occurrence also increased to 60% at 530 °C when the concentration of methanol in the droplets was increased to 10% with the same initial droplet size of 130 µm. Also, the probabilities of microexplosion occurrence were 30% at 500 ℃ and 40% at 560 ℃.

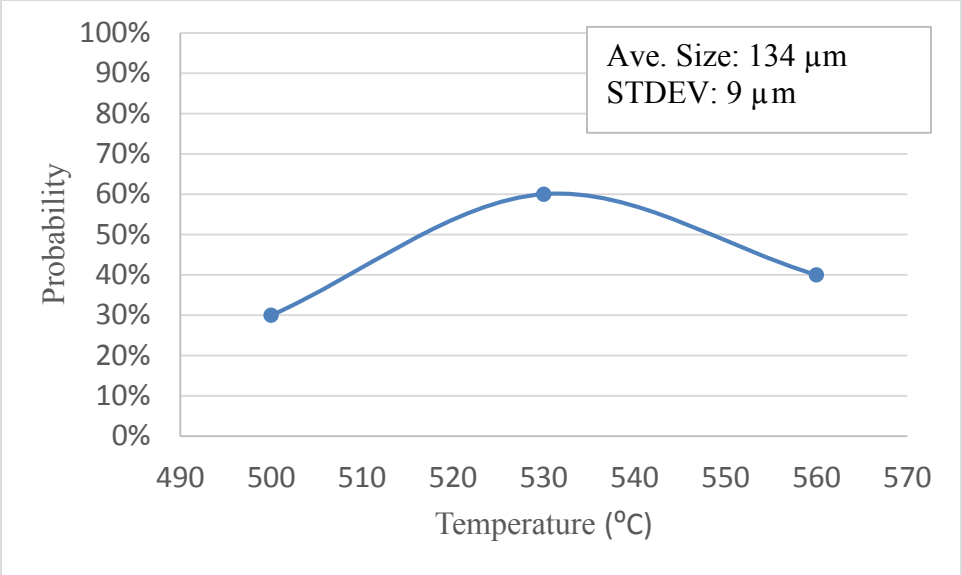

Figure 22. Probability of microexplosion of GM 90/10 mixtures with 134 µm of initial droplet size.

Lastly, the concentration of methanol in methanol-in-glycerol mixture droplets was increased to 15%. The probability of microexplosion occurrence of GM 85/15 mixtures is shown in 23. The average initial droplet size was 225 µm with a standard deviation of 9 µm. The highest probability of microexplosion occurrence was 90% at 630 ℃. It happened at the lower temperature compared to the GM 90/10 with 223 µm of initial droplet size. Also, the probabilities of microexplosion occurrence were 60% at 600 ℃ and 70% at 660 ℃.

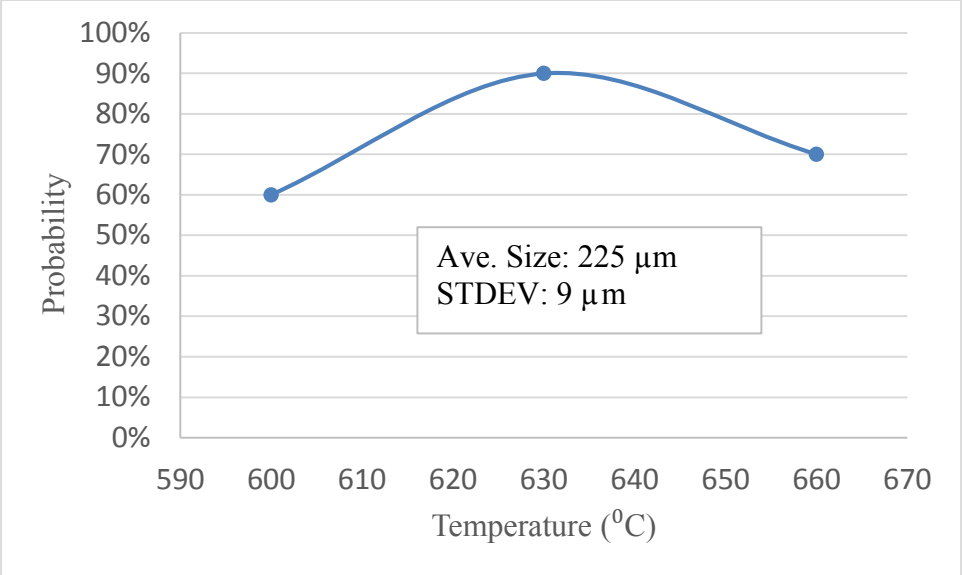

Figure 23. Probability of microexplosion of GM 85/15 mixtures with 225 µm of initial droplet size.

The probability of microexplosion occurrence of GM 85/15 mixtures with smaller droplets is shown in Figure 24. The average initial droplet size was 137 µm with a standard deviation of 8 µm. The highest probability of microexplosion occurrence was 60% at 470 ℃. It happened at the lower temperature compared to GM 90/10 with 134 µm of initial droplet size. Also, the probability of microexplosion occurrence was 40% when temperature were 440 ℃ and 500 ℃.

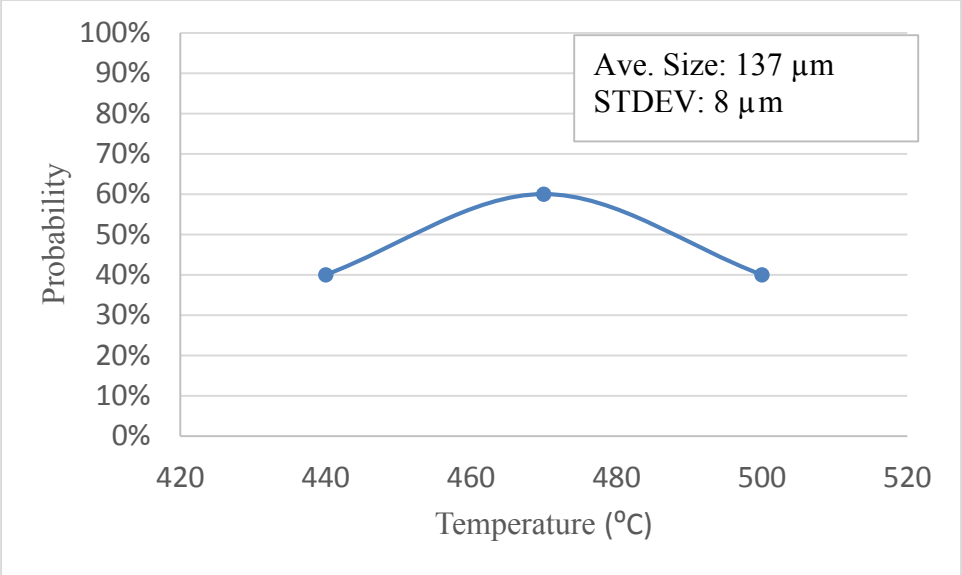

Figure 24. Probability of microexplosion of GM 85/15 mixtures with 137 µm of initial droplet size.

The highest probability of microexplosion occurrence happened at different temperatures, depending on the conditions (i.e. size and concentration of methanol) of the droplets. As it can be seen in the figures, the highest probability of microexplosion occurred at an optimum temperature point. It is hypothesized that when the temperatures were very high, the vaporization rate of methanol within a droplet was greater than the bubble nucleation rate, which led to methanol vaporization or combustion before reaching conditions conducive for microexplosion. On the other hand, when the temperatures were very low, the bubble nucleation rate was slower than the vaporization rate of the droplets, which also led to complete vaporization of methanol before microexplosion could take place. This is consistent with results obtained by Mikami et al. [9]. The results also suggest that microexplosion takes place when the bubble nucleation rate is high enough to allow the inner pressure of the droplets to build up rapidly before methanol is able to evaporate.

Table 7 shows the highest probability of microexplosion occurrence in all methanol-in-glycerol mixtures.

Table 7. Probability of microexplosion in methanol-in-glycerol mixtures

Mixture Type	Initial Droplet Size (μm)	Temperature (°C)	Probability of Microexplosion
GM 95/5	222	680	70%
	136	530	40%
GM 90/10	223	680	90%
	134	530	60%
GM 85/15	225	630	90%
	137	470	60%

The Effect of Methanol Concentration on Probability of Microexplosion Occurrence

The concentration of methanol is an important factor that affects the probability of microexplosion occurrence. Methanol-in-glycerol mixtures with 5%, 10% and 15% methanol were tested in the combustion chamber. Figures 25 and 26 show the highest probability of microexplosion occurrence in methanol-in-glycerol mixtures with two different initial droplet sizes, 230 μm and 130 μm. Both figures show the same trend of probability. The probability of microexplosion increased when the concentration of methanol increased from 5% to 10%. This is because more methanol within the droplets leads to more bubble nucleation sites [10]. Bubble nucleation is a necessary condition for microexplosion of droplets [5]. Also, the highest probability of microexplosion took place at a lower temperature when the concentration of methanol increased to 15%. This is because the effective superheat limit of droplets depends on the mole fraction of methanol

as observed by Mikami et al. [9]. Therefore, droplets with greater amount of methanol should reach the superheat limit at lower temperatures.

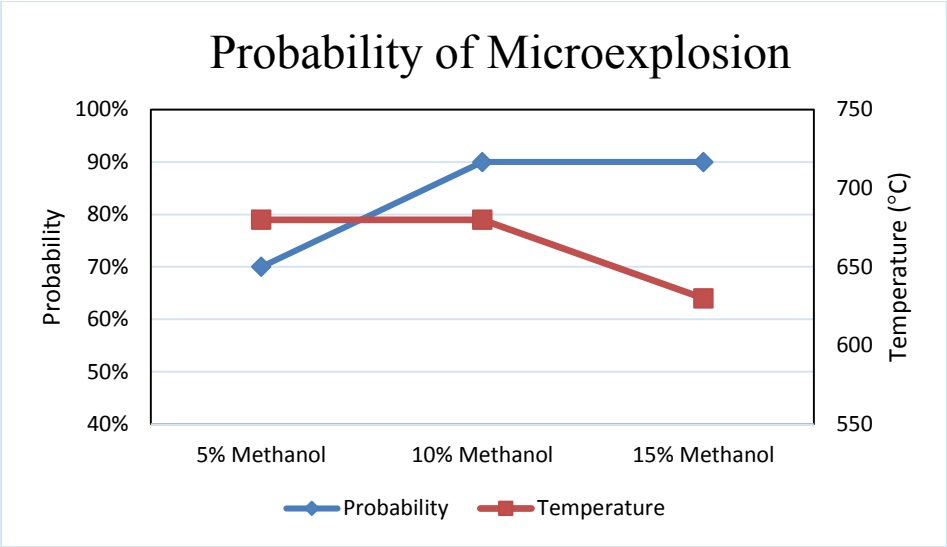

Figure 25. The effect of methanol concentration on the probability of microexplosion of methanol-in-glycerol mixtures with 230 µm of droplet size.

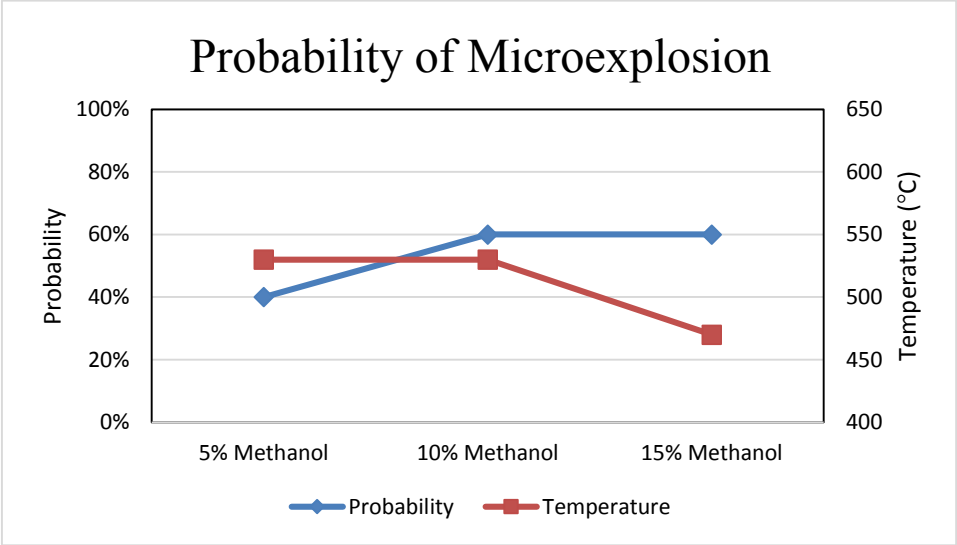

Figure 26. The effect of methanol concentration on the probability of microexplosion of methanol-in-glycerol mixtures with 130 µm of droplet size.

The Effect of Initial Droplet Size on Probability of Microexplosion Occurrence

A droplet's initial size is also an important factor that affects the probability of microexplosion occurrence. Two initial droplet sizes, 130 μm and 230 μm, were tested in the experiment. Figure 27 shows that 230 μm as the initial droplet size has higher probability of microexplosion occurrence than the 130 μm droplets in three different concentrations of mixtures. Smaller droplets have higher surface-to-volume ratio resulting in stronger vaporization at high temperatures [27]. On the other hand, most of 230 μm droplets size microexploded if the concentration of methanol was 10% or 15%. Furthermore, once the droplets reached a methanol concentration of 10%, the probability of microexplosion remained constant, which suggests that a minimum amount of methanol is needed to ensure proper microexplosion. Moreover, once the minimum amount is exceeded, nucleation time seems to increase which also could lead to lower nucleation rate. The combined effect usually leads to an optimum probability of microexplosion as seen in other binary mixtures [9].

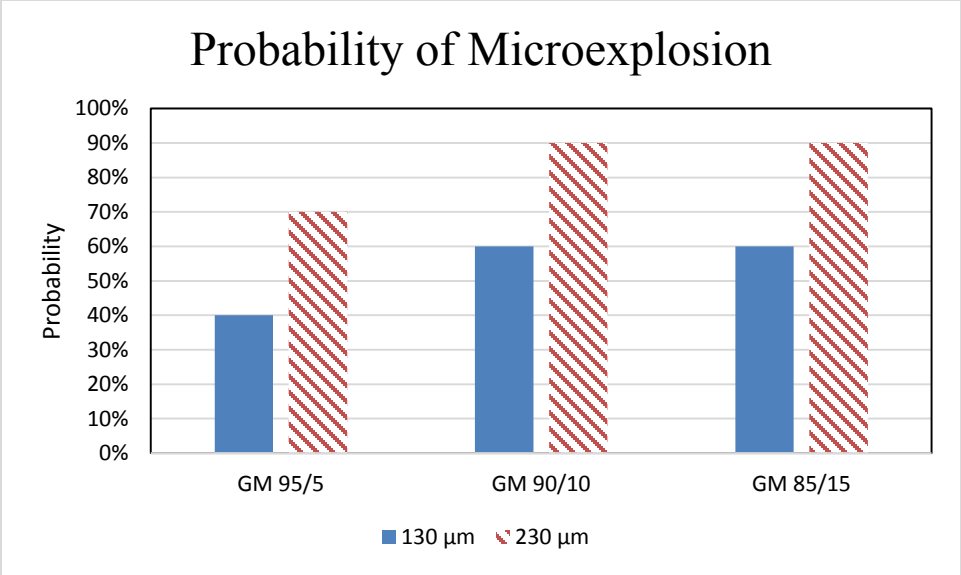

Figure 27. The effect of initial droplet size on the probability of microexplosion of methanol-in-glycerol mixtures.

5.1.2 Water-in-Glycerol Mixtures

Probability of Microexplosion Occurrence of GW 50/50 Mixtures

The water-in-glycerol mixture droplets were tested in order to compare the results of the methanol-in-glycerol mixture droplets. The probability of microexplosion occurrence of GW 50/50 mixtures is shown in Figure 28. The average initial droplet size was 228 µm with a standard deviation of 10 µm. The highest probability of microexplosion occurrence was 80% at 560 ℃. Also, the probabilities of microexplosion occurrence were 60% at 530 ℃ and 40% at 610 ℃.

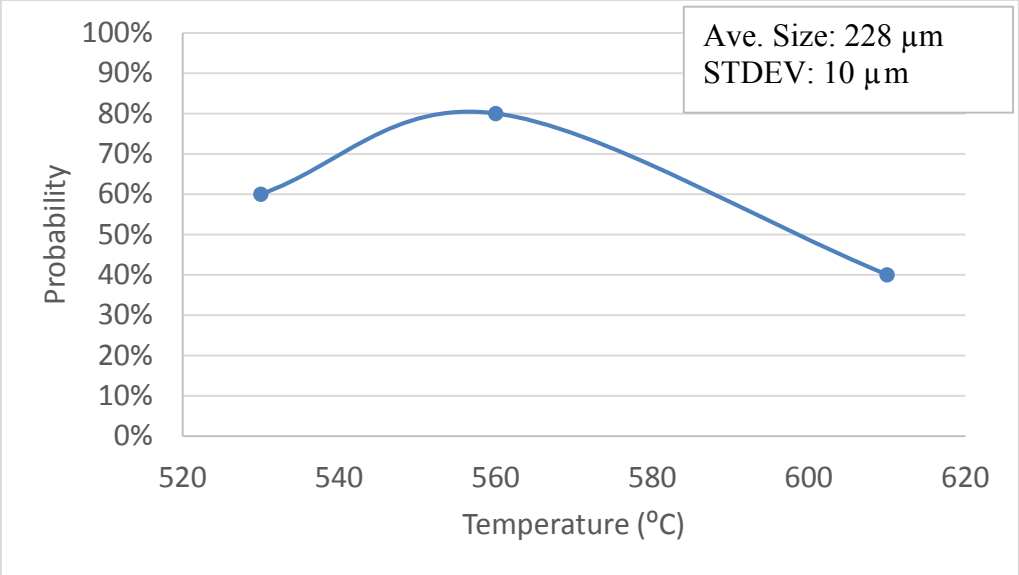

Figure 28. Probability of microexplosion of GW 50/50 mixtures with 228 µm of average initial droplet size.

The probability of microexplosion occurrence of GW 50/50 mixtures with smaller droplets is shown in Figure 29. The average initial droplet size was 135 µm with a standard deviation of 9 µm. The highest probability of microexplosion occurrence was 60% at 510 °C because of the small sizes of the droplets. Also, the probabilities of microexplosion occurrence were 30% at 470 °C and 20% at 550 °C.

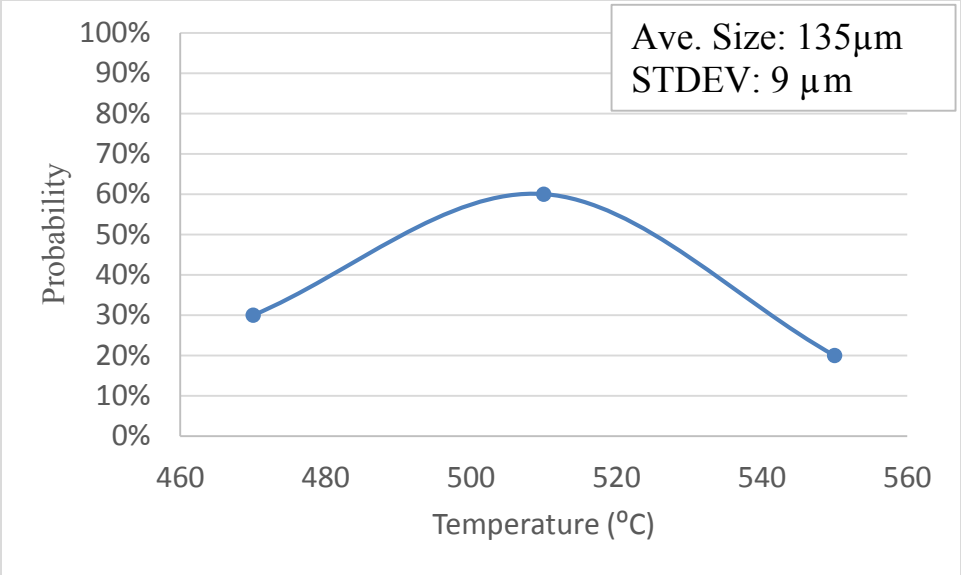

Figure 29. Probability of microexplosion of GW 50/50 mixtures with 135 µm of average initial droplet size.

The highest probability of microexplosion occurrence happened at two different temperatures due to different initial droplet sizes. Furthermore, the droplets vaporized at high temperatures since the vaporization rate of water within a droplet was expected to be faster than the bubble nucleation rate as in the case of methanol-glycerol mixtures. Also, the bubble nucleation rate was slower than the vaporization rate of the droplet at low temperatures, resulting in droplet vaporization, which is consistent with the results reported by Mikami et al. [9]. Table 8 shows the highest probability of microexplosion occurrence in water-in-glycerol mixtures.

Table 8. Probability of microexplosion in water-in-glycerol mixtures

Mixture Type	Initial Droplet Size (μm)	Temperature (°C)	Probability of Microexplosion
GW 50/50	228	560	80%
	135	510	60%

The Effect of Water Concentration and Initial Droplet Size on Probability of Microexplosion Occurrence

Water-in-glycerol mixtures with 15% water were tested to observe microexplosion phenomena. However, no microexplosion was observed during the droplet lifetime for droplets with an initial droplet size of 230 μm. Since water has a higher boiling point than methanol, the difference in volatility and boiling point between water and glycerol is smaller than methanol and glycerol. Therefore, the concentration of water should be increased to 50% in order to induce and observe microexplosion.

In addition, the initial droplet size had a great effect on the probability of microexplosion in water-in-glycerol mixtures as well. Figure 30 shows that droplets with an initial droplet size of 230 μm had higher probability of microexplosion occurrence than the 130 μm droplets. Also, the smaller droplets microexploded at lower temperatures compared to the bigger droplets since a smaller droplet has a higher surface-to-volume ratio. The higher surface-to-volume ratio results in stronger evaporation at high temperatures [27].

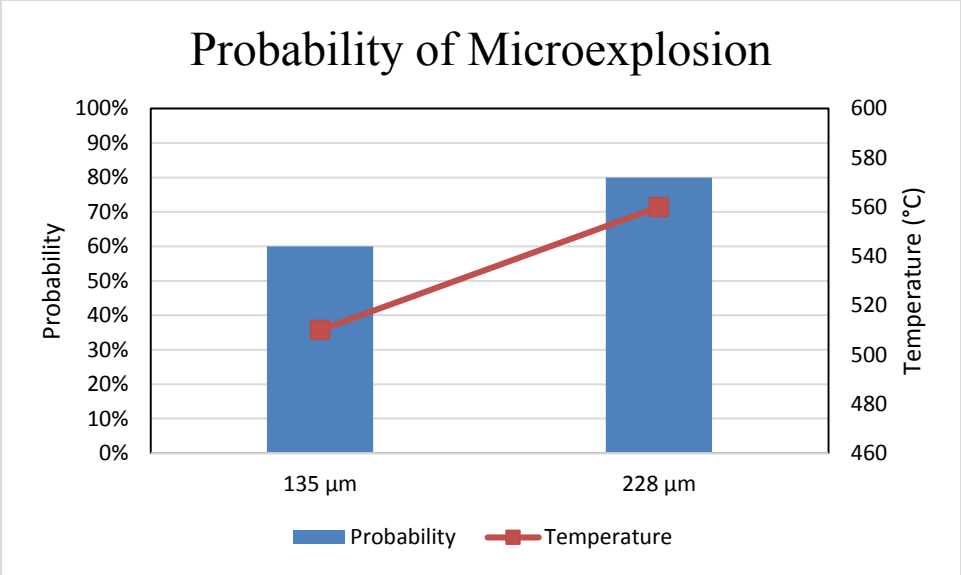

Figure 30. The probability of microexplosion occurrence of water-in-glycerol mixtures.

5.2 Acoustic Signal Analysis

Acoustic waves of microexplosion were collected using an acoustic sensor when the highest probability of microexplosion occurred. A Fast Fourier Transform (FFT) algorithm was used to analyze the collected data using Matlab to identify the characteristic frequencies of microexplosion. In addition, a pencil lead break test was used to synchronize the high speed camera images with the acoustic data collected using the acoustic emission sensor system. The pencil lead break test was used to ensure the transducers worked perfectly, and to determine the noise frequencies associated with the experimental set up.

5.2.1 Noise Frequency

Noise frequencies were found by using a pencil lead break test in order to identify and differentiate frequencies of microexplosion while running the experiments [21]. Ten pencil lead break tests were conducted on the sensor, the platinum stick, the platinum wire and the whole assembly so that the noise frequencies could be analyzed statistically. The four setups are shown in Figure 31. The frequencies with above 50% probability, which are shown in Table 9, were regarded as noise frequencies.

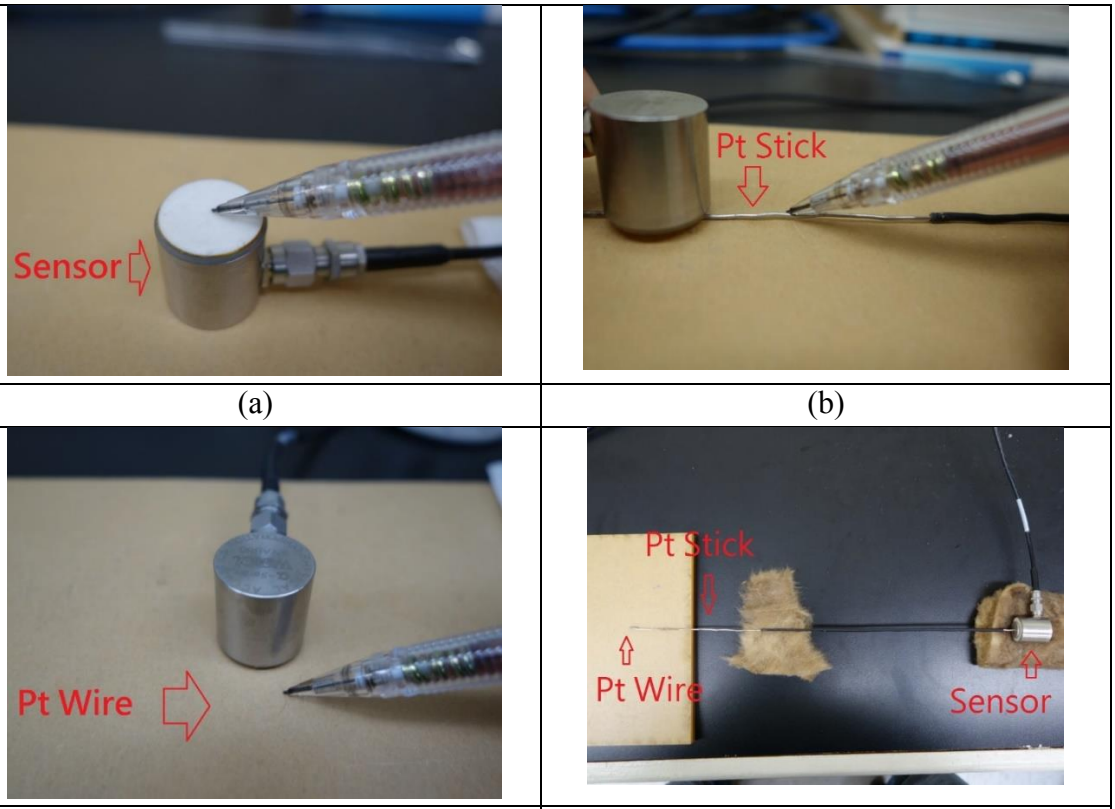

Figure 31. Pencil lead break test setups, (a) test on the sensor (b) test on the platinum stick (c) test on the platinum wire (d) test on the platinum wire that is attached to platinum stick.

Table 9. Noise frequencies of the transducers

(a) Sensor		(b) Pt Stick		(c) Pt Wire		(d) Whole Part	
Freq. (kHz)	Pr.	Freq. (kHz)	Pr.	Freq. (kHz)	Pr.	Freq. (kHz)	Pr.
39	**100%**	30	20%	**40**	**80%**	16	10%
65	10%	**39**	**90%**	64	20%	**24**	**90%**
73	**100%**	70	40%	66	10%	**28**	**60%**
83	10%	**73**	**100%**	70	40%	32	10%
112	20%	115	10%	**73**	**60%**	50	40%
119	**90%**	118	10%	84	20%	55	20%
146	20%	144	20%	119	30%	178	40%
152	20%	146	10%	**144**	**60%**		
165	10%	**170**	**80%**	149	30%		
197	20%			170	10%		

In addition, the noise frequencies of the cooling pipe were also filtered out when analyzing the frequency of microexplosion. As shown in Figure 32, the noise frequencies were 0-100 kHz, 105 kHz, 120 kHz, 150 kHz, 185 kHz and 220 kHz.

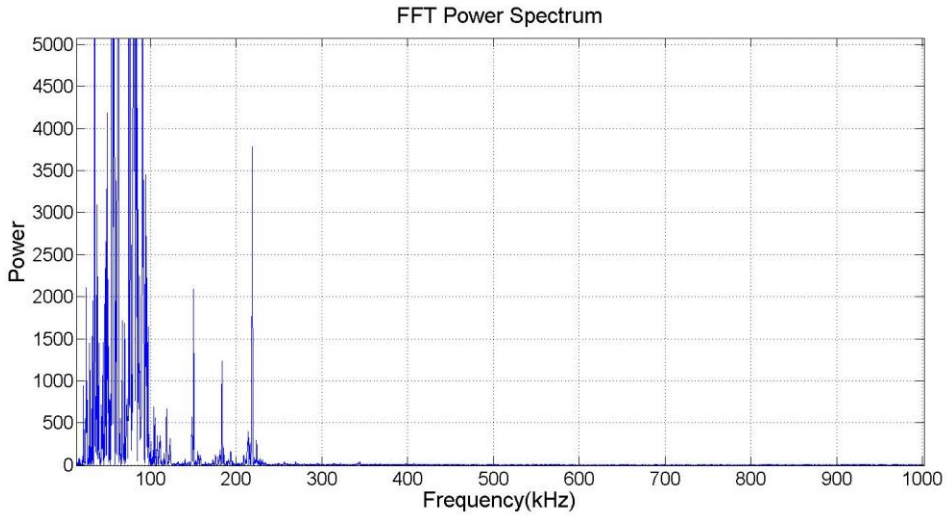

Figure 32. Noise frequency of cooling pipe

5.2.2 Analysis of Microexplosion of Methanol-in-Glycerol Mixtures

Six combinations of droplet sizes and methanol-in-glycerol mixture concentrations were considered at the temperatures characterized by having the highest probability of microexplosion. The microexplosion experiments of GM 95/5 mixture with droplet size of 143 μm was performed at 530 ℃. Figure 33 shows that the droplet expanded until 0.285 seconds and microexploded into smaller droplets at 0.286 seconds or 1 ms later. The time response and frequency response of GM 95/5 mixture with droplet size of 143 μm at 530 ℃ are shown in Figure 34 After filtering out the noise frequencies of the platinum wire, the platinum stick and the cooling pipe, the greatest power of frequency was consider as the characteristic microexplosion frequency. The characteristic microexplosion frequency of the droplet was 210 kHz.

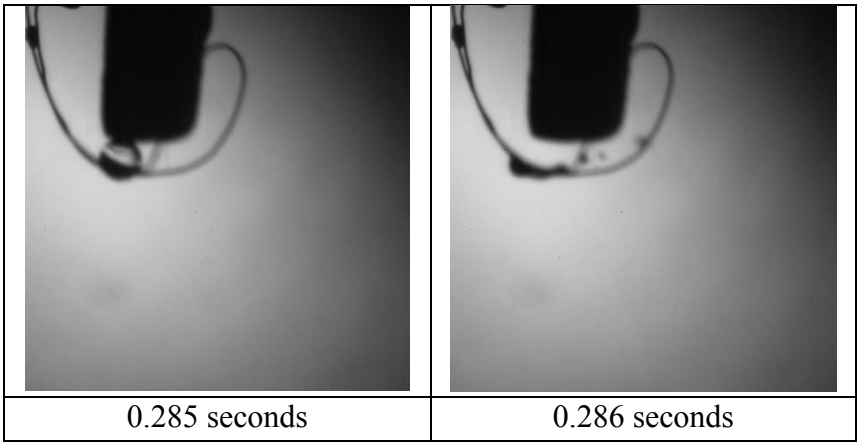

Figure 33. GM 95/5 mixture droplet of 143 μm at 530 ℃.

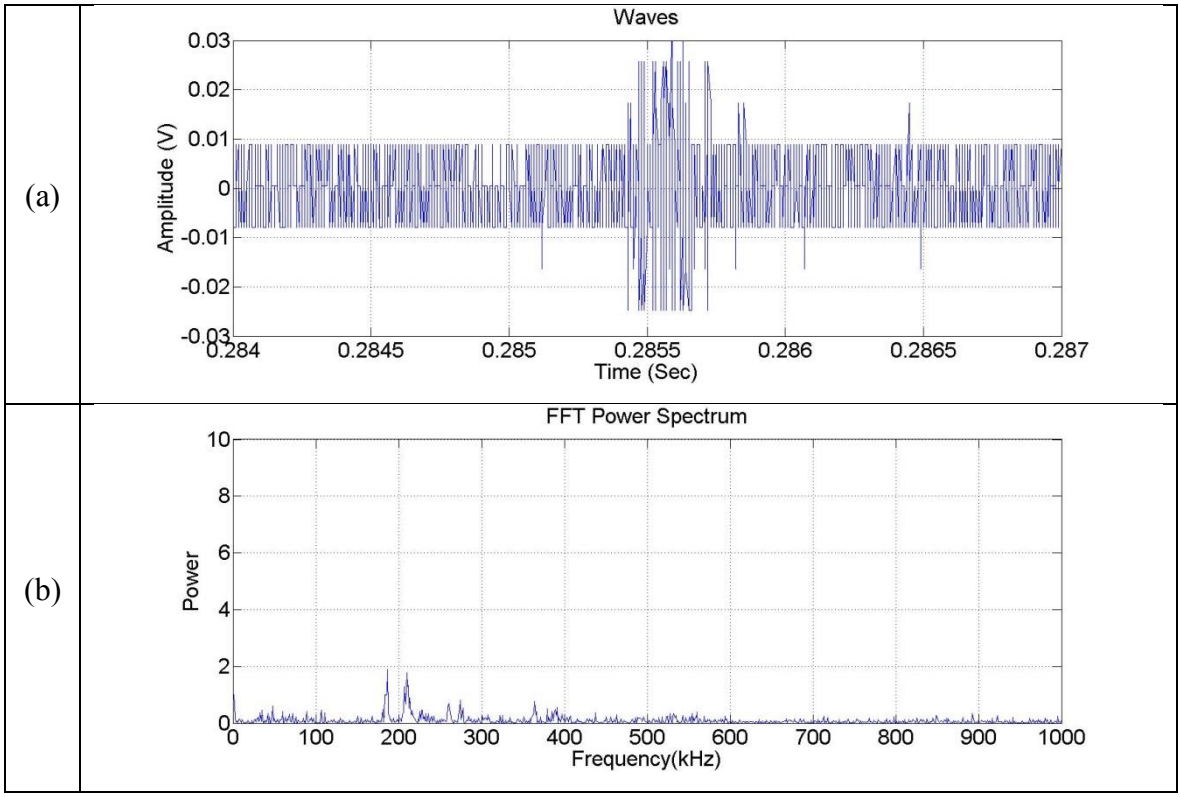

Figure 34. Microexplosion of GM 95/5 mixture droplet of 143 μm at 530 ℃
(a) time response (b) frequency response.

The microexplosion experiments of GM 95/5 mixture with droplet size of 223 μm was conducted at 680 ℃. As shown in Figure 35, the droplet expanded until 0.110 seconds and exploded at 0.111 seconds or 1 ms later. Figure 36 (a) shows the wave signals for the droplet. The frequency spectrum of the droplet is shown in Figure 36 (b) obtained using the Fast Fourier Transform algorithm. After filtering out the noise frequencies, the characteristic microexplosion frequency of GM 95/5 mixture with droplet size of 223 μm at 680 ℃ was 200 kHz.

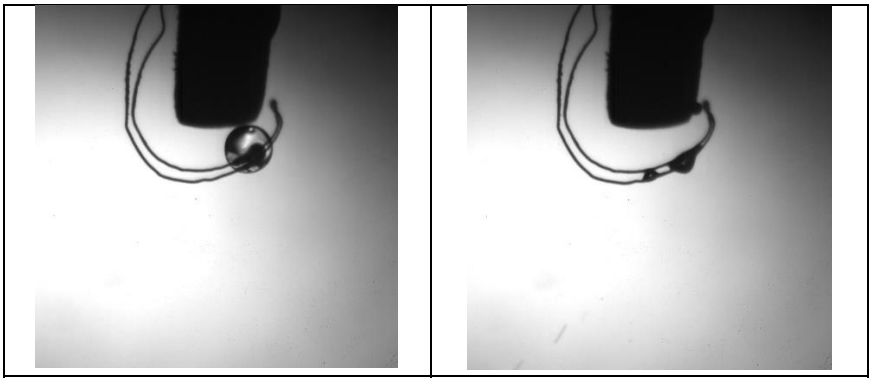

0.110 seconds	0.111 seconds

Figure 35. GM 95/5 mixture droplet of 223 μm at 680 ℃.

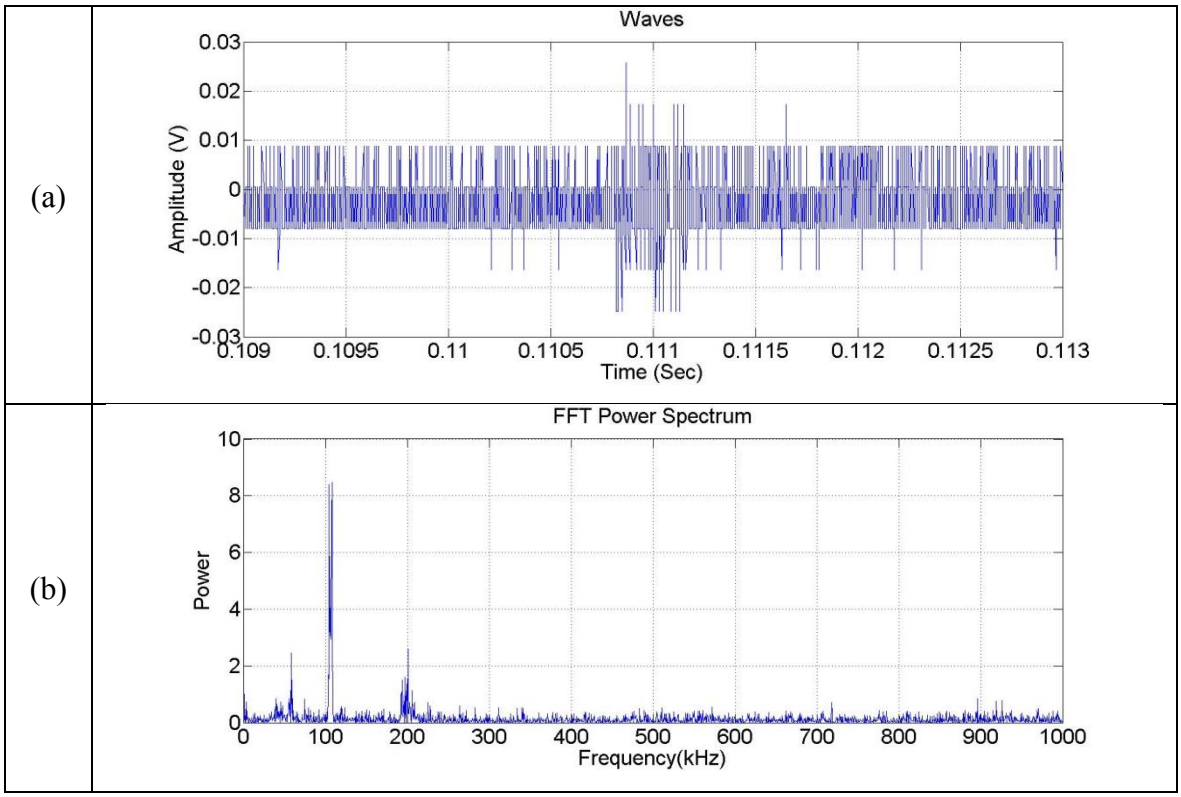

Figure 36. Microexplosion of GM 95/5 mixture droplet of 223 μm at 680 ℃ (a) time response (b) frequency response.

The microexplosion experiment of GM 90/10 mixture with droplet size of 144 μm was conducted at 530 °C. As shown in Figure 37, the droplet expanded until 0.480 seconds, and exploded into smaller droplets at 0.481 seconds. Figure 38 shows the wave signals and frequency spectrum of the droplet. The characteristic microexplosion frequency of GM 90/10 mixture with droplet size of 144 μm was 385 kHz.

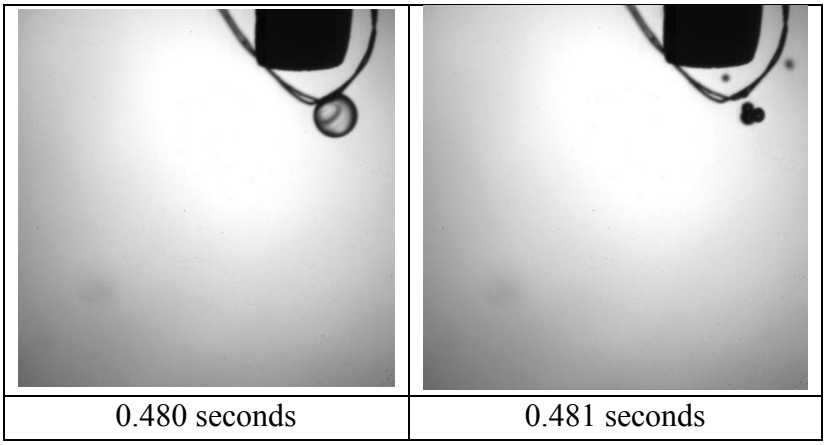

0.480 seconds	0.481 seconds

Figure 37. GM 90/10 mixture droplet of 144 μm at 530 °C.

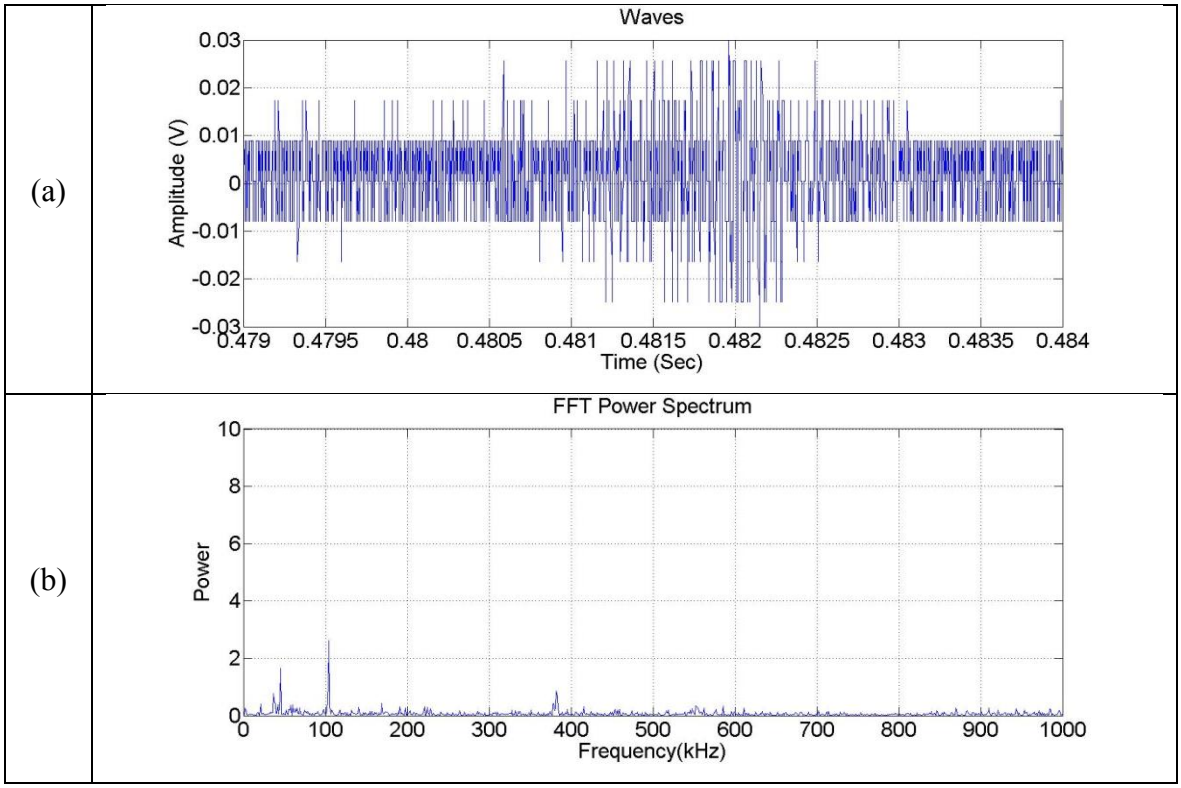

Figure 38. Microexplosion of GM 90/10 mixture droplet of 144 μm at 530 ℃
(a) time response (b) frequency response.

The microexplosion experiment of GM 90/10 mixture with droplet size of 230 μm was performed at 680 ℃. Figure 39 shows that the droplet exploded at 0.388 seconds. The time response and frequency response of GM 90/10 mixture with droplet size of 230 μm at 680 ℃ are shown in Figure 40. The characteristic microexplosion frequency of the droplet was 360 kHz after filtering out the noise frequencies.

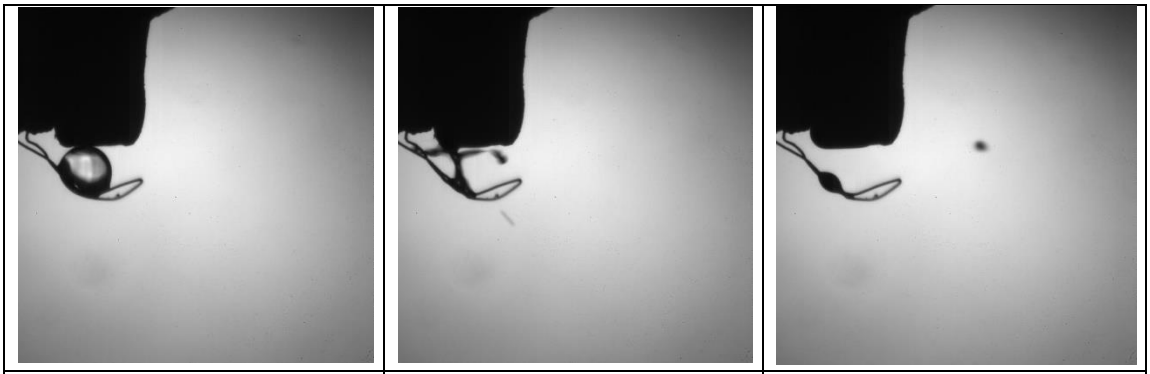

0.387 seconds	0.388 seconds	0.389 seconds

Figure 39. GM 90/10 mixture droplet of 230 μm at 680 ℃.

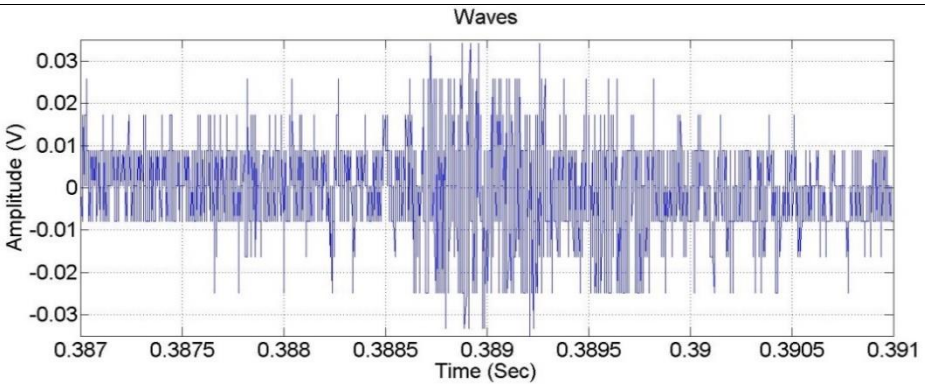

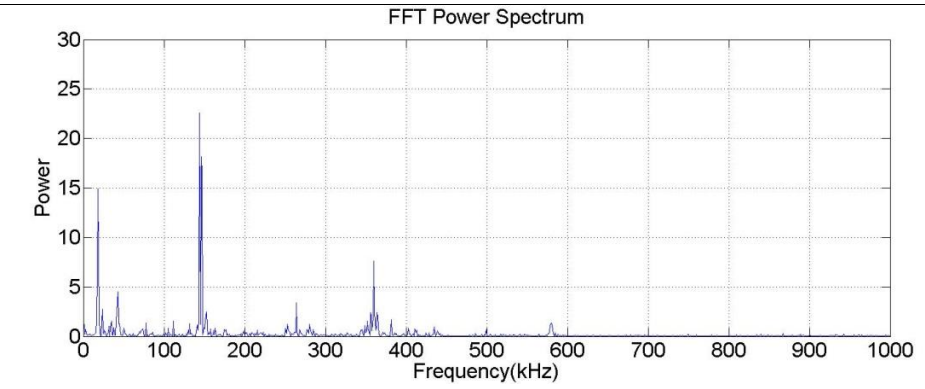

Figure 40. Microexplosion of GM 90/10 mixture droplet of 230 μm at 680 ℃
(a) time response (b) frequency response.

The microexplosion experiment of GM 85/15 mixture with droplet size of 138 μm was conducted at 470 °C. As depicted in Figure 41, the droplet expanded until 0.373 seconds, and partially exploded at 0.374 seconds. Figure 42 shows the wave signals and frequency spectrum of the droplet. The characteristic microexplosion frequency of GM 85/15 mixture with droplet size of 138 μm was 540 kHz after filtering out noise frequencies.

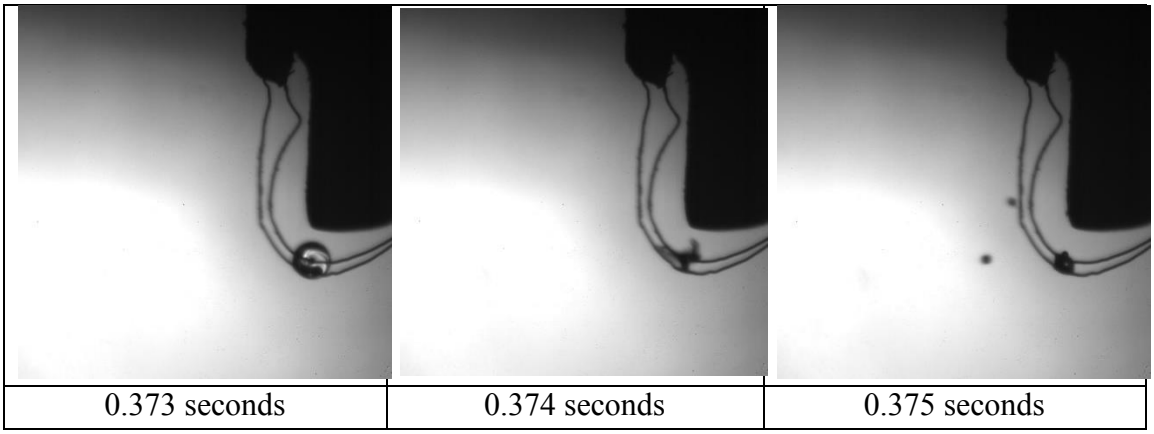

0.373 seconds	0.374 seconds	0.375 seconds

Figure 41. GM 85/15 mixture droplet of 138 μm at 470 °C.

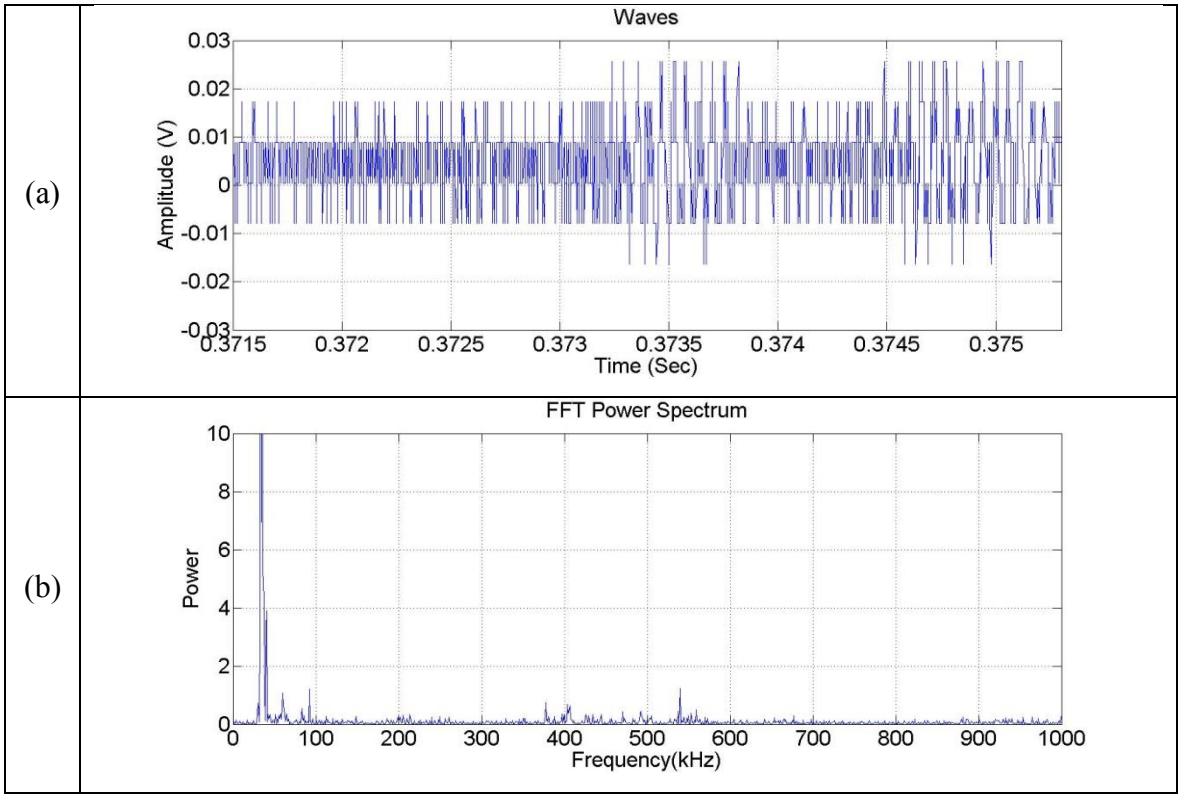

Figure 42. Microexplosion of GM 85/15 mixture droplet of 138 μm at 470 ℃
(a) time response (b) frequency response.

The microexplosion experiment of GM 85/15 mixture with droplet size of 236 μm was conducted at 630 °C. As shown in Figure 43, the droplet expanded until 0.571 seconds, and partially exploded at 0.572 seconds. Figure 44 shows the wave signals and frequency spectrum of the droplet. The characteristic microexplosion frequency of the GM 85/15 mixture with droplet size of 236 μm was 455 kHz.

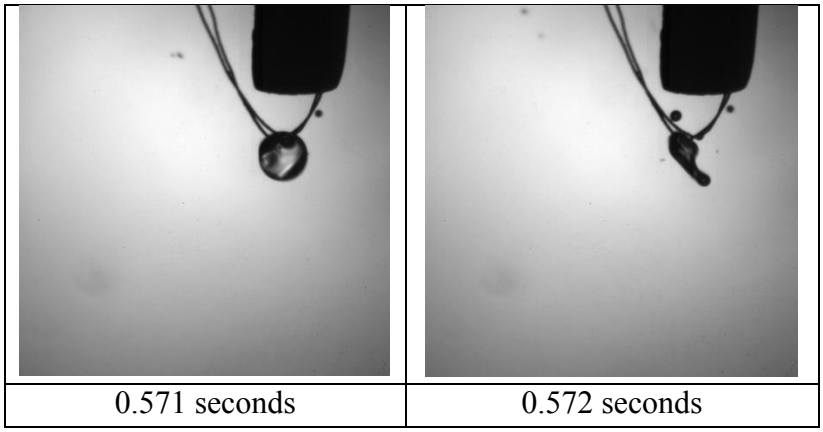

0.571 seconds	0.572 seconds

Figure 43. GM 85/15 mixture droplet of 236 μm at 630 °C.

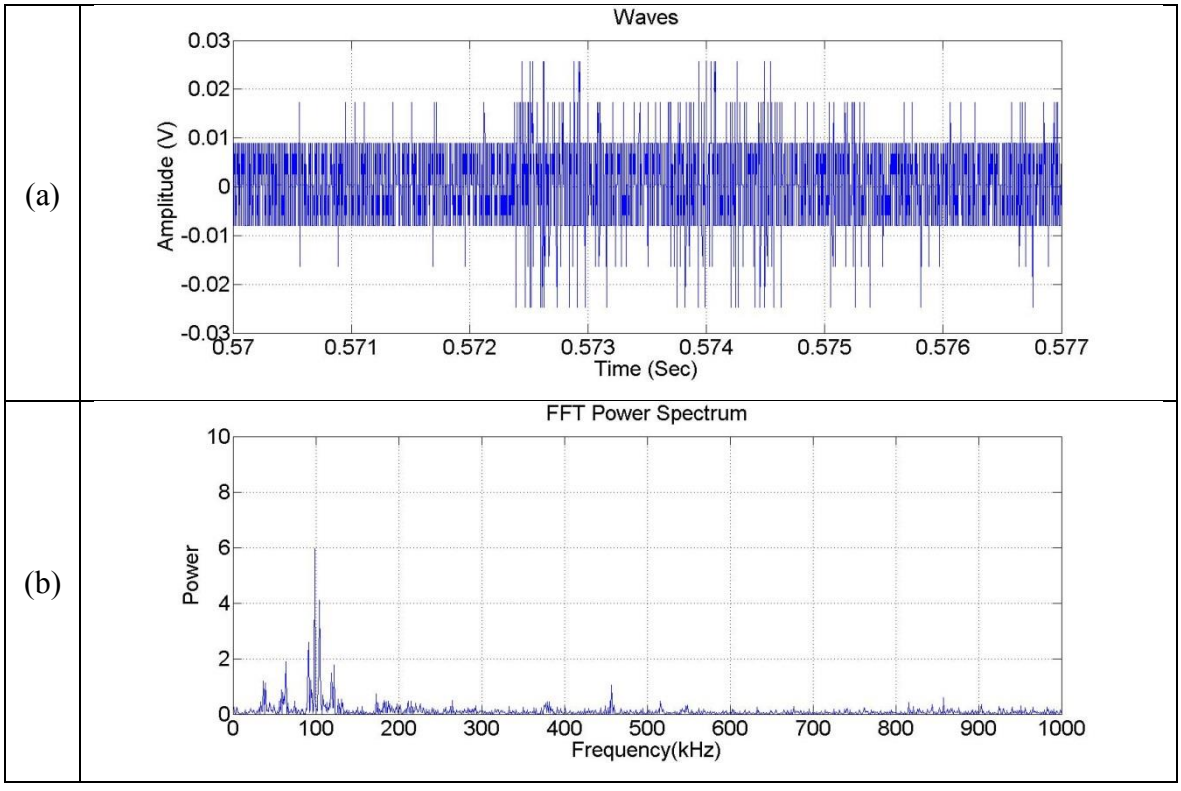

Figure 44. Microexplosion of GM 85/15 mixture droplet of 236 μm at 630 ℃
(a) time response (b) frequency response.

Table 10. Characteristic microexplosion primary frequencies of methanol-in-glycerol mixtures

Mixture Type	Initial droplet size (μm)	Temperature (°C)	Characteristic frequency (kHz)
GM 95/5	143	530	210
	223	680	200
GM 90/10	144	530	385
	230	680	360
GM 85/15	138	470	540
	236	630	455

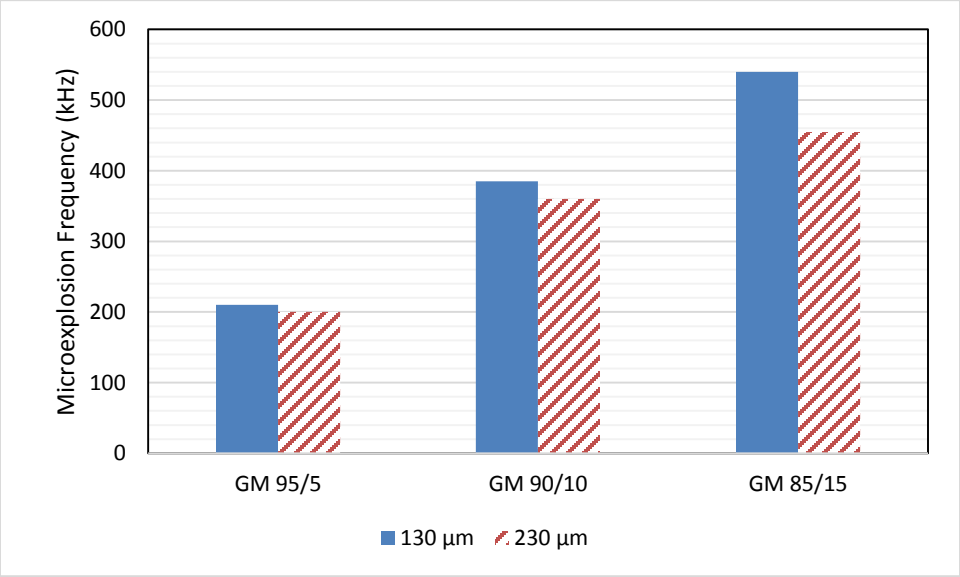

Figure 45. Characteristic frequency of microexplosion of methanol-in-glycerol mixtures.

The characteristic microexplosion frequencies of methanol-in-glycerol mixture droplets are shown in Table 8. As shown in Figure 45, the characteristic microexplosion frequencies of the 230 μm droplets were lower than that of the 130 μm droplets when the concentration of methanol in mixtures were the same. In addition, the characteristic microexplosion frequencies increased with an increase in the concentration of methanol

in the methanol-in-glycerol mixture droplets. In order to understand the relationship between the characteristic frequency of microexplosion and the droplet properties, the strength of a microexplosion and its corresponding frequency should be postulated explicitly.

According to Nam [24], a partial differential equation (PDE) can be used to characterize the wave motion caused by microexploded droplet suspended at the tip of a long elastic bar (stick) [28] as shown in Figure 46.

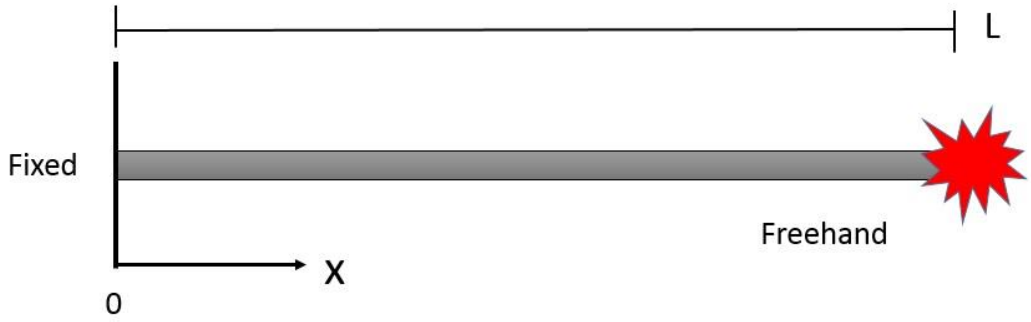

Figure 46. Elastic bar with fixed and freehand conditions under the effect of microexplosion [24].

The strength of the force generated by the microexplosion effect can be evaluated by solving the wave equation (6) by considering the following conditions:

$$\frac{\partial^2 u}{\partial t^2} = a^2 \frac{\partial^2 u}{\partial x^2} \tag{6}$$

where, $a = \sqrt{\frac{E}{\rho}}$ is the longitudinal wave speed (m/s)

E is the elastic modulus

Conditions:

$u(0,t)=0$, for no displacement at $x=0$

$\frac{\partial u}{\partial x}(L,t)=0$, for no displacement gradient at free end at $x=L$

$u(x,0)=0$, for no initial displacement at $t=0$

$\frac{\partial u}{\partial t}(x,0)=\frac{Ft'}{m}$, for the impulse at $t=0$

Equation (7) is the solution for Equation (6) after taking into account all the conditions including the impulse force generated by microexplosion. As it can be seen in the equation (7), the force generated by microexplosion is directly proportional to displacement of the long bar (i.e. stick). Therefore, it is evident that stronger strength of microexplosion should result in larger displacements.

$$u(x,t)=\sum_{n=0}^{\infty} C_n' \sin\left(\sqrt{\lambda}x\right)\sin\left(a\sqrt{\lambda}t\right) \tag{7}$$

where, $C_n'=\frac{2}{L}\cdot\frac{Ft'}{m}\int_0^L \sin\left(\sqrt{\lambda}x\right)dx$

$\lambda=\left(\frac{(2n+1)\pi}{2L}\right)^2$ n=1, 2, 3…

F is the constant total net force (N)

t' is the time interval over the impulse force (s)

m is the constant mass of the object (kg)

u (x ,t) is the displacement (m)

Because the acoustic sensor can measure the period of the impulse wave generated by microexplosion, the period of wave of the long bar can be obtained. The sound wave velocity can be obtained by using Equations (8) and (9). Also, the relationship between the frequency and the displacement is shown in Equation (10), which suggests that smaller displacements lead to the higher frequencies. Furthermore, smaller explosive force (or smaller displacement) as shown in Equation (7), leads to higher frequency of microexplosion.

$$\frac{u(x,t)}{T} = \frac{1}{T}\sum_{n=0}^{\infty} C_n' \cos\left(\sqrt{\lambda}x\right)\sin\left(a\sqrt{\lambda}t\right) \tag{8}$$

where, *T* is the total period of impulse wave (s)

$$\frac{u(x,t)}{T} = v \tag{9}$$

$$f = \frac{v}{u(x,t)} \tag{10}$$

where, *f* is frequency (Hz)

v is the sound wave velocity (m/s)

The effect of droplet properties on the strength of each microexplosion event can be understood better by using the model proposed by Fu et al. [29]. Fu et al. [29] developed a model of microexplosion for water-in-oil emulsified droplets, which can be used to describe the strength of microexplosion numerically. The definition of microexplosion strength K is shown in Equation (11).

$$K = \int_0^{R_1} \left(4\pi r^2 \phi J\right) M dr \tag{11}$$

where, $M = 4/3\pi\left(R_0^3 - r^3\right)\rho$ is the mass of a droplet [kg]

J is the nucleation rate of a droplet [$1/m^3s^1$]

ϕ is volume fraction of water in an emulsified droplet

R_0 is the initial radius of emulsion droplet [m]

R_1 is the radius of emulsion kernel when oil membrane is formed [m]

According to the homogeneous nucleation theory [30], a fast growth rate of nucleation happens when the droplet temperature reaches the superheat limit. The definition of the nucleation rate shown in Equation (11), J, is shown in Equation (12).

$$J = n_T \frac{kT}{h} \exp\left(-\frac{4\pi r_{cr}^2 \gamma}{3kT}\right) \tag{12}$$

where, n_T is the number of potential nucleation sites per unit volume

k is the Boltzmann's constant (1.3808×10^{-23} J/K)

h is the Planck's constant (6.6261×10^{-34} J·s)

r_{cr} is the critical diameter of a vapor embryo (m)

γ is the surface tension (kg/s^{-2})

In the microexplosion experiments of methanol-in-glycerol mixtures, the results show that the larger initial droplet size led to lower characteristic microexplosion frequency when the droplets had the same concentration of methanol. This phenomenon can be explained by considering the magnitude of microexplosion force (or strength) in Equations (7), (10) and (11). From Equation (11), it is evident that larger initial droplet size leads to stronger strength (or force) of microexplosion which result in lower microexplosion frequencies according to Equations (7) and (10). Therefore, the characteristic microexplosion frequency should be lower in the larger methanol-in-glycerol mixture droplets.

The observed microexplosion frequencies of methanol-in-glycerol mixture droplets were higher at greater concentrations of methanol in the droplets. This seems to contradict the model of microexplosion strength (Equation (11)), which predicts that more water in a droplet should lead to a stronger microexplosion effect. However, the secondary fluid used in this research was methanol and not water, which has higher surface tension as shown in Table 11. Furthermore, the surface tension of glycerol is higher than that of methanol, which suggests that greater concentration of methanol would result in lower surface tension of the droplets. In addition, low surface tension leads to low contact angle of droplets. As shown in Table 12, GM 85/15 droplets have lower contact angle on the

original (uncoated) and coated foils compared to GM 95/5 droplets. It confirms that more methanol in droplets results in lower surface tension as it can be predicted by the Young's equation used to determine surface tension of droplets on surfaces as follows:

$$\cos(\theta) = \frac{\gamma_{solid-gas} - \gamma_{solid-liquid}}{\gamma_{liquid-gas}} \quad (13)$$

Where, θ, $\gamma_{solid\text{-}gas}$, $\gamma_{solid\text{-}liquid}$ and $\gamma_{liquid\text{-}gas}$ are the contact angle, surface tension between the gas and liquid phases, surface tension between the solid and liquid phases, and surface tension between liquid and gas phases, respectively.

Table 11. Surface tension of fluids

		Fluid	**Surface Tension [dyne/cm] @20°C**
Fu et al. Model	Base Fluid	Diesel[a]	25.8
	Secondary Fluid	Water[b]	72.75
Experiment	Base Fluid	Glycerol[c]	63.2
	Secondary Fluid	Methanol[b]	22.95
[a]-Reference [31], [b]-Reference [32], [c]-Reference [33]			

Table 12. Contact angle of methanol-in-glycerol mixture droplets on platinum foil

Droplets Type	**Droplet contact angle on original platinum foil**	**Droplet contact angle on coated platinum foil**
GM 95/5	60.4°	96.1°
GM 90/10	59.9°	90.3°
GM 85/15	59.9°	87.4°

Again, the effect of surface tension on microexplosion strength can be evaluated by examining Equations (11) and (12), which suggest that lower surface tension should

lead to stronger microexplosion. So the only explanation for the observed behavior lies on the assumption than droplets with lower surface tension requires smaller internal pressures to counteract its surface tension, which leads to incomplete or partial microexplosion of droplets. In such a scenario, the strength of the microexplosion phenomena would be notably less pronounced since not all the high-vapor pressure (or low boiling point) fluid would contribute to microexplosion as envisioned by Equations (11) and (12). Figures 41 and 43 show GM 85/15 mixture droplets (droplets with 15% methanol) that partially microexploded, which were characterized by having a weak microexplosion given the high frequencies detected by the acoustic sensor. Further studies are necessary to determine the effect of low surface tension on the strength of microexplosion.

5.2.3 Analysis of Microexplosion of Water-in-Glycerol Mixtures

The microexplosion experiments of water-in-glycerol mixture with two different sizes were conducted at temperatures when the highest probability of microexplosion happened. As shown in Figure 47, the droplet of GW 50/50 with droplet size of 134 μm was conducted at 510 °C, and microexploded into many smaller droplets at 0.390 seconds. Also, the droplet of GW 50/50 with droplet size of 242 μm was performed at 560 ℃ as seen in Figure 49. Figure 48 and 50 are the time and frequency responses of two GW 50/50 mixture droplets.

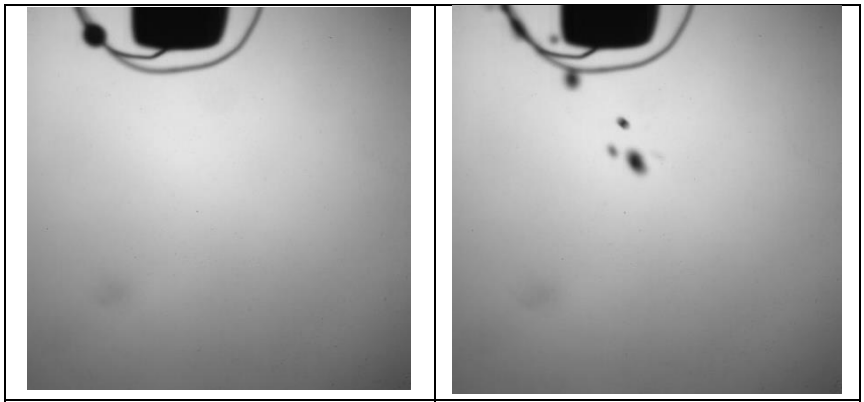

0.389 seconds	0.390 seconds

Figure 47. GW 50/50 mixture droplet of 134 μm at 510 °C.

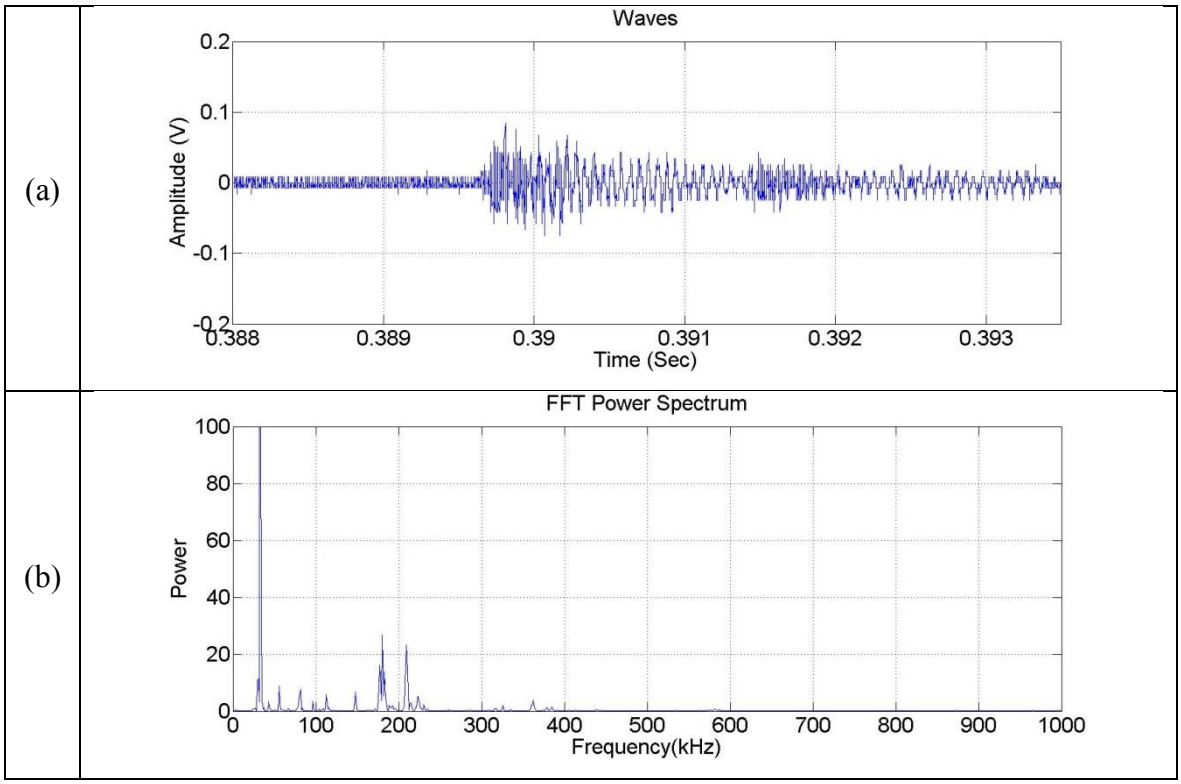

Figure 48. Microexplosion of GW 50/50 mixture droplet of 134 μm at 510 ℃
(a) time response (b) frequency response.

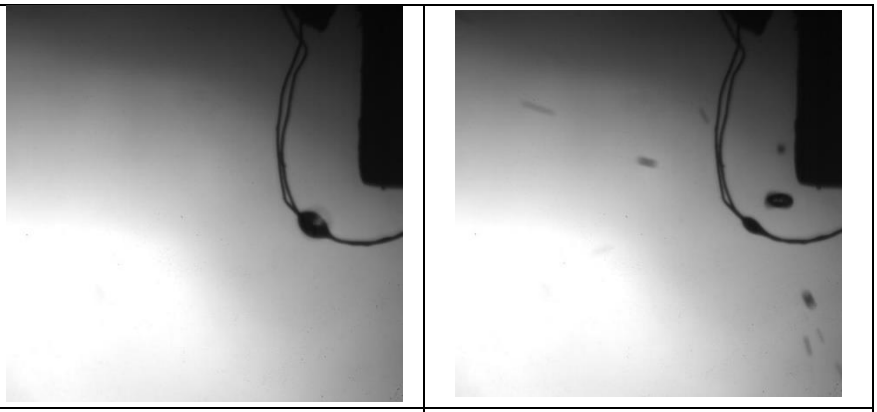

0.109 seconds	0.110 seconds

Figure 49. GW 50/50 mixture droplet of 242 μm at 560 °C.

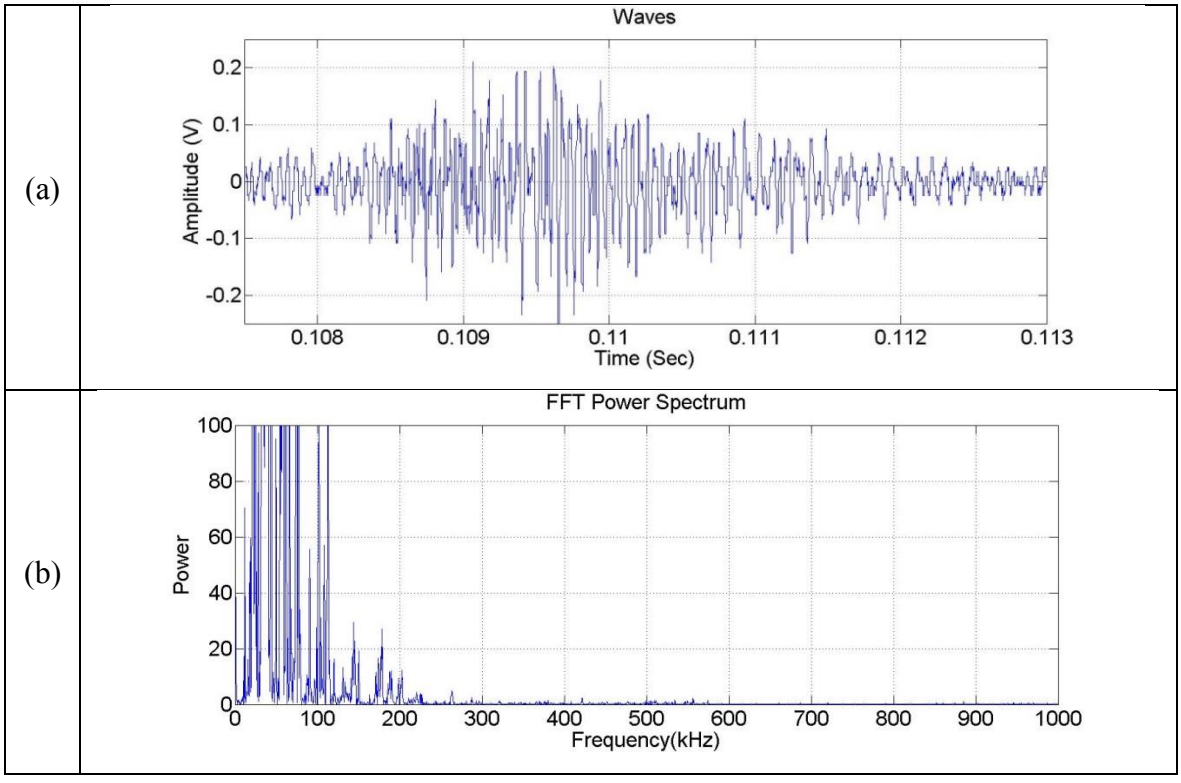

Figure 50. Microexplosion of GW 50/50 mixture droplet of 242 μm at 560 ℃
(a) time response (b) frequency response.

The characteristic microexplosion frequencies of water-in-glycerol mixture droplets are shown in Table 13. As seen in Figure 51, the characteristic microexplosion frequency of the droplets of 242 µm was lower than that of the droplet of 134 µm. Thus, the effect of initial droplet size on the characteristic frequency is similar as in the cases of methanol-in-glycerol mixture droplets. Also, the characteristic frequencies confirm the fact that a larger droplet leads to stronger strength of microexplosion, resulting in the low characteristic microexplosion frequency.

Table 13. Characteristic microexplosion frequency of water-in-glycerol mixtures.

Mixture Type	Initial droplet size (µm)	Temperature (°C)	Characteristic frequency (kHz)
GW 50/50	134	510	210
	242	560	180

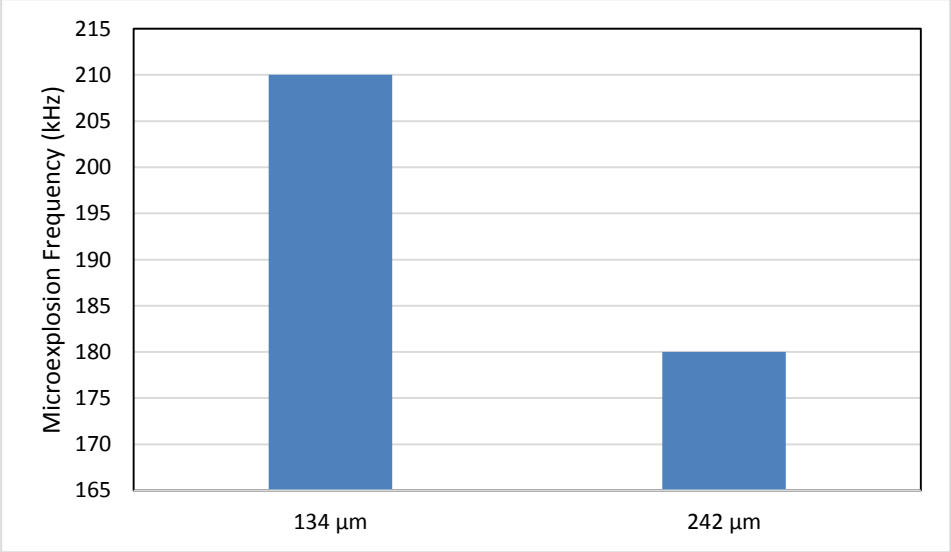

Figure 51. Characteristic frequency of microexplosion of water-in-glycerol mixtures

5.2.4 The Effect of Monomolecular Base Fuel on Characteristic Microexplosion Frequency

For methanol-in-glycerol and water-in-glycerol mixture droplets, experimental observation revealed a single characteristic microexplosion frequency for each droplet condition as shown in Table 10 and Table 13. In addition, the characteristic microexplosion frequency for each droplet condition (size and content) was found to be consistent after running several microexplosion experiments. This clearly indicates that the predictable and rather constant strength of microexplosion mainly depends on droplet condition. Therefore, it can be inferred that when the chemical composition of droplets is well prescribed using monomolecular fluids, microexplosion can take place in a rather predictable manner. On the other hand, multiple characteristic microexplosion frequencies were found when testing droplets of methanol-in-canola oil mixtures [24], which are characterized by having a significant number of hydrocarbon molecules with different molecular weights. This is particularly true in the case of canola oil since it exhibits multiple characteristic microexplosion frequencies for identical droplet sizes. In summary, a single characteristic microexplosion frequency was found for each droplet condition when using glycerol as a monomolecular liquid as base fuel.

6. CONCLUSION

Through this research project, the best fuel conditions were found for the highest probability of microexplosion occurrence of GM 95/5, GM 90/10, GM 85/15, and GW 50/50 mixture droplets with two initial droplet sizes, 130 μm and 230 μm, respectively. In addition, the relationship between the microexplosion acoustic response and the droplet properties was studied. The major conclusions of this research project are mentioned below.

6.1 The Probability of Microexplosion Occurrence

1. In the case of methanol-in-glycerol mixture droplets, higher concentration of methanol in droplets leads to higher probability of microexplosion occurrence. More methanol results in more bubble nucleation sites, which is a necessary condition for microexplosion of droplets.
2. The highest probability of microexplosion occurrence took place at a lower temperature when the concentration of methanol in droplet was 15%. Since superheat limit depends on the mole fraction of methanol, the droplets were able to reach the superheat limit at lower temperatures.
3. For all mixtures, smaller droplets had lower probability of microexplosion occurrence than larger droplets. This was because the smaller droplets had higher surface-to-volume ratio resulting in stronger vaporization at high temperatures.

6.2 Signal Analysis of Microexplosion

1. In methanol-in-glycerol mixture droplets, the characteristic microexplosion frequency increased with an increase in the concentration of methanol in the droplets. More methanol in the droplets led to the weaker strength of the microexplosion due to lower surface tension of droplets which led to incomplete or partial microexplosion.
2. For all mixtures, smaller droplets produced higher frequencies when the concentration of secondary fluid (methanol and water) in the droplets were the same. Smaller droplets led to weaker strength of microexplosion resulting in the higher frequencies.
3. A single characteristic microexplosion frequency was found for each droplet condition when using glycerol as a monomolecular liquid as base fuel.

REFERENCES

[1] M. Heming, Glycerine market report, HB International SAS, 2012.

[2] M. Bohon, B. Metzger, W. Linak, C. King, W. Roberts, Glycerol combustion and emission, Proceedings of the Combustion Institute 33 (2011) 2717-2724.

[3] V.M. Ivanov, P.I. Nefdov, Experimental investigation of the combustion process in nature and emulsified fuels, NASA TT F-258 (1965).

[4] C.K. Law, Recent advances in droplet vaporization and combustion, Prog. Energy Combust. Sci. 8, 171-201 (1982).

[5] C.K. Law, Combustion Physics, Cambridge University Press, Cambridge, 2006.

[6] T. Houlihan, The triple crown, Power Engineering 4 (2009) 44-45.

[7] T. Kadota, H. Yamasaki, Recent advances in the combustion of water fuel emulsion, Progress in Energy and Combustion Science 28 (2002) 385-404.

[8] F.L. Dryer, Water addition to practical combustion systems - concepts and applications, International Symposium on Combustion 16 (1977) 279-295.

[9] M. Mikami, T. Yagi, N. Kojima, Occurrence probability of microexplosion in droplet combustion of miscible binary fuels, Proc. Combust. Inst. 27 (1998) 1933-1941.

[10] M. Tsue, T. Kaota, D. Segawa, H. Yamasaki, Statistical analysis on onset of microexplosion for an emulsion droplet, International Twenty-Sixth Symposium on Combustion, The Combustion Institute (1996) 1629-1635.

[11] H. Watanabe, T. Harada, K. Hoshino, Y. Matsushita, H. Aoki, T. Miura, An experimental investigation of the characteristics of the secondary atomization and spray combustion for emulsified fuel, Journal of Chemistry Engineering 41 (2008) 1110-1118.

[12] L. Ferrante, M. Miccio, F. Miccio, R. Solimene, Fluidized bed combustion of liquid biofules: Application of integrated diagnostics for microexplosions characterization, Energy & Fuels 22 (2008) 4213-4222.

[13] C.H. Wang, C.K. Law, Microexplosion of fuel droplets under high pressure, Combustion and Flame 59 (1985) 53-62.

[14] W. Hsieh, R. Chen, C. Chen, S. Chiu, T. Lin, Micro-explosion of a water-in-hexadecane compound drop, Journal of the Chinese institute of engineers, 35;5, 579-587

[15] C. Grosse, M. Ohtsu, Acoustic Emission Testing, Springer- Verlag Berlin Heidelberg, Germany, 2008.

[16] H. Vallen, AE testing fundamentals, equipment, and applications, Journal of Nondestructive Testing (Germany) 7 (2002) 1-30.

[17] AE Sensors & Preamplifiers Users Manual, Part no. 1220-1001, Physical Acoustics Corporation, Princeton, New Jersey, 2002.

[18] NI-SCOPE Software User Manual, Part no. 322808A-01, National Instruments Corporation, Austin, Texas, 2001.

[19] W. Cochran, J. Cooley, D. Favin, H. Helms, R. Kaenel, W. Lang, G. Maling, D. Nelson, C. Rader, P. Welch, What is the Fast Fourier Transform, Proceedings of the IEEE, 55 (1967) 1664-1674.

[20] Christian Grosse, Hsu-Nielsen Source, NDT.net, Germany, "Available: http://www.ndt.net/ndtaz/content.php?id=474", (1 Dec. 2011).

[21] J. Yu, P. Ziehl, B. Zarate, J. Caicedo, L. Yu, V. Giurgiutiu, B. Metrovich, F. Matta, Quantification of fatigue cracking in CT specimens with passive and active piezoelectric sensing, Proceedings of SPIE 7649 (2010) 76490R-1.

[22] H. Yamasaki, Y. Obata, H. Nomura, Y. Ujie, Analytical study on microexplosion processes of a burning emulsion droplet using acoustic emission, Nihon Kikai Gakkai Nenji Taikai Koen Ronbunshu 3 (2005) 125-126.

[23] J. Tanaka, S. Nakajima, K. Tanaka, C.Y. Kim, K. Korematsu, Study on microexplosion of a droplet of emulsified fuel and its acoustic emission, Transactions of the Japan Society of Mechanical Engineers B 68, (2002) 1302-1307.

[24] Hyungseok Nam, An Experimental Investigation of Microexplosion in Emulsified Vegetable-Methanol Blend, Thesis of Master of Science, Texas A&M University, (2012).

[25] Aculon 905 Product Information, Aculon Inc., San Diego, California, 2012.

[26] Aculon E Product Information, Aculon Inc., San Diego, California, 2012.

[27] C. Shen, W. L. Cheng, K. Wang, C. F. Lee, Estimating the secondary droplet size distribution after microexplosion of bio-fuel droplets, ILASS-Americas 22nd Annual Conference on Liquid Atomization and Spray Systems, Cincinnati, OH, May 2010.

[28] M.C. Potter, J.L. Goldberg, E. Aboufadel, Advanced Engineering Mathematics: Third edition, Oxford University Press, Oxford, 2005.

[29] W.B. Fu, L.Y. Hou, L. Wang, F.H. Ma, A unified model for the microexplosion of Emulsified droplets of oil and water. Fuel Processing Technology 79 (2002) 107-119.

[30] M.W. Rohsenow, J.P. Hartnett, E.N. Ganić, Handbook of Heat Transfer Fundamentals: 2nd edition, McGraw-Hill, New York, 1985.

[31] A.B. Chhetri, K.C. Watts, Surface tension of petro-diesel, canola, jatropha and soapnut biodiesel fuels at elevated temperature and pressures, Fuel, 104 (2013) 704-710

[32] G. Va´zquez, E. Alvarez, J. Navaza, Surface Tension of Alcohol + Water from 20 to 50 °C., J. Chem. Eng. Data, 40 (1995) 611-614.

[33] F. E. Bartell, J. W. Shepard, Surface roughness as related to hysteresis of contact angles, J. Phys. Chem., 57 (1953) 455-458

APPENDIX A

MATLAB CODE OF FAST FOURIER TRANSFORM

The following Matlab code [24] was used to analyze collecting data from NI USB 5132. The Fast Fourier Transform (FFT) algorithm was also used in this code in order to determine the microexplosion frequencies.

```
load GM95_1.txt ;                    % Load wave signal data
f1=    GM95_1   (:,1);               % Time
f2=    GM95_1   (:,2);               % Amplitude

% Plot signal waves on time domain
Plot (f1, f2), grid, title ('Waves' , 'fontsize', 24);
xlabel ('Time (Sec)' , 'fontsize', 24)
ylabel ('Amplitude (V) ' , 'fontsize', 24)

Y = fft(f2);      % Returns the discrete Fourier transform (DFT) of vector x, computed
with a fast Fourier transform algorithm

N = length(Y);                       % length of N value
Y(1) = [];
```

```
power = abs(Y(1:N/2)).^2;                % Fine single-sided spectrum by using abs
function
freq = (1:N/2)/(N/2).*1000;              % Fine frequency points

% Plot single-sided amplitue spectrum
plot (freq , power), grid on
xlabel ('Frequency(kHz)' , 'fontsize', 24)
ylabel ('Power' , 'fontsize', 24)
title ('FFT Power Spectrum' , 'fontsize', 24)

% Save frequency data
z=[freq', power];
save GM95_1 z /ascii
pause
```